Title

Observations and models of emissions of volatile terpenoid compounds from needles of ponderosa pine trees growing in situ: control by light, temperature and stomatal conductance

Journal

Oecologia, 176(1)

ISSN

0029-8549

Authors

Harley, Peter
Eller, Allyson
Guenther, Alex
et al.

Publication Date

2014-09-01

DOI

10.1007/s00442-014-3008-5

Oecologia (2014) 176:35–55
DOI 10.1007/s00442-014-3008-5

PHYSIOLOGICAL ECOLOGY - ORIGINAL RESEARCH

Observations and models of emissions of volatile terpenoid compounds from needles of ponderosa pine trees growing in situ: control by light, temperature and stomatal conductance

Peter Harley · Allyson Eller · Alex Guenther · Russell K. Monson

Received: 3 March 2014 / Accepted: 25 June 2014 / Published online: 12 July 2014

Abstract Terpenoid emissions from ponderosa pine (*Pinus ponderosa* subsp. *scopulorum*) were measured in Colorado, USA over two growing seasons to evaluate the role of incident light, needle temperature, and stomatal conductance in controlling emissions of 2-methyl-3-buten-2-ol (MBO) and several monoterpenes. MBO was the dominant daylight terpenoid emission, comprising on average 87 % of the total flux, and diurnal variations were largely determined by light and temperature. During daytime, oxygenated monoterpenes (especially linalool) comprised up to 75 % of the total monoterpenoid flux from needles. A significant fraction of monoterpenoid emissions was dependent on light and $^{13}CO_2$ labeling studies confirmed de novo production. Thus, modeling of monoterpenoid emissions required a hybrid model in which a significant fraction of emissions was dependent on both light and temperature, while the remainder was dependent on temperature alone. Experiments in which stomata were forced to close using abscisic acid demonstrated that MBO and a large fraction of the monoterpene flux, presumably linalool, could be limited at the scale of seconds to minutes by stomatal conductance. Using a previously published model of terpenoid emissions, which explicitly accounts for the physicochemical properties of emitted compounds, we were able to simulate these observed stomatal effects, whether induced experimentally or arising under naturally fluctuation conditions of temperature and light. This study shows unequivocally that, under naturally occurring field conditions, de novo light-dependent monoterpenes comprise a significant fraction of emissions in ponderosa pine. Differences between the monoterpene composition of ambient air and needle emissions imply a significant non-needle emission source enriched in Δ-3-carene.

Keywords BVOC emissions · Monoterpenes · 2-Methyl-3-buten-2-ol · ^{13}C labeling · Linalool

Introduction

The importance of biogenic volatile organic compounds (BVOC) in tropospheric chemistry is widely

Communicated by Joy K. Ward.

Electronic supplementary material The online version of this article (doi:10.1007/s00442-014-3008-5) contains supplementary material, which is available to authorized users.

P. Harley (✉) · A. Guenther
National Center for Atmospheric Research, Boulder, CO 80301, USA
e-mail: harley@ucar.edu

Present Address:
P. Harley
Estonian University of Life Sciences, Tartu 51014, Estonia

A. Eller
Cooperative Institute for Research in Environmental Sciences, University of Colorado, Boulder, CO 80301, USA

A. Eller
Macquarie University, NSW 2109, Australia

Present Address:
A. Guenther
Pacific Northwest National Laboratory, Richland, WA 99352, USA

R. K. Monson
School of Natural Resources and the Environment and the Laboratory for Tree Ring Research, University of Arizona, Tucson, AZ 85721, USA

acknowledged, with BVOC playing important roles in tropospheric O_3 production and the formation and growth of secondary organic aerosol. In order to quantify the role of BVOCs in local photochemistry and oxidation processes, it is important to characterize the composition, magnitude, and controls over emission dynamics at the scale of individual needles, so that this information can be incorporated into existing models of BVOC emissions at larger scales. Emissions of isoprene, the dominant emitted BVOC in many forest ecosystems, depend on both leaf temperature and incident irradiance and are independent of changes in stomatal conductance. This behavior is captured well in existing models (Guenther et al. 2012; Martin et al. 2000; Zimmer et al. 2000). The precise nature of environmental control over other terpenoid species is less well characterized. Emission of monoterpenes arising from specialized storage structures within the leaf have been generally assumed to depend solely on leaf temperature, while an increasing number of tree species have been shown to produce monoterpenes de novo and emit them in a light and temperature dependent manner, analogous to that of isoprene (Staudt and Seufert 1995). More recently, Ghirardo et al. (2010) demonstrated that even in species with specialized storage structures, a varying fraction of emissions arises from de novo production rather than diffusion from storage. Laboratory experiments have also shown that certain terpenoid species may be limited by stomatal conductance under conditions that were not steady state (Niinemets et al. 2002, 2003a) This is an effect not currently incorporated into BVOC emission models. This study attempts to clarify, under natural field conditions, the roles of needle temperature, incident light, and varying stomatal conductance in controlling terpenoid emissions of ponderosa pine, which is a widely distributed and ecologically significant species.

This study was undertaken in conjunction with two field campaigns, BEACHON-ROCS in 2010 and BEACHON-ROMBAS in 2011, which addressed the important role of BVOC emissions from a forest of *Pinus ponderosa* in gas phase and particle-phase processes, respectively (Ortega et al. 2014). BVOCs at the site are dominated by local emissions arising from ponderosa pine, which we estimate to comprise over 99 % of the tree biomass.

Above-canopy BVOC flux measurements at the site using eddy covariance techniques coupled to both PTR–MS and PTR–TOF–MS (Kaser et al. 2013a, b) cannot distinguish between compounds of the same mass, thus precluding speciation of important families of BVOC such as monoterpenes and sesquiterpenes. Gas chromatography–mass spectrometry (GC–MS) techniques used to measure air mixing ratios and fluxes above the canopy using relaxed eddy accumulation may underestimate BVOC species emitted in low amounts or highly reactive species with short lifetimes because the magnitude of individual compound fluxes may fall below the detection limit. Due to these shortcomings of measurements above the canopy, emission measurements at the scale of needles have an important role in these large field campaigns by identifying a more complete suite of emitted compounds, particularly those that are highly reactive and emitted at modest rates, and those which may play a role in photochemistry disproportionate to their emission fluxes. Marked differences between emissions observed at the needle scale and mixing ratios observed in the air space above the canopy provide information about chemical processing within the canopy or additional nonfoliar sources of BVOC.

Additionally, needle emission data provide the best means of describing the physical and biological controls over emissions. A particular focus of this study is the degree to which incident photosynthetic photon flux density (PPFD) influences monoterpene emissions in ponderosa pine, and in particular, whether different monoterpene species respond differently. A related question involves the importance of stomatal conductance in regulating these emissions. Niinemets and Reichstein (2003a) and subsequent studies have confirmed that, under certain conditions, and depending on the physico-chemical characteristics of the BVOC in question, stomata can play a role in limiting emissions. Since stomatal conductance generally correlates with incident light, care must be taken to distinguish between direct effects of light on monoterpene production and indirect effects on emissions resulting from changes in stomatal conductance. In this study, we addressed these issues using measurements of BVOC emission rates that were coupled with detailed compound identification and characterization of needle physiology on trees during two growing seasons. We made a special effort to identify environmental and physiological controls over needle BVOC emissions that have been poorly characterized in past emission models.

Materials and methods

Site description

The Manitou Experimental Forest Observatory (39.1006°N, 105.0942°W; ranging from 2,280 to 2,840 m a.s.l.), was established in 2008 under the auspices of the National Center for Atmospheric Research in Boulder, CO, and is located within the U.S. Forest Service Manitou Experimental Forest, approx. 45 km northwest of Colorado Springs, Colorado. It has been the site of several interdisciplinary studies examining the role of

biogenic trace gas emissions on gas phase and particle-phase processes in the local atmosphere (Ortega et al. 2014). The forest is a pine savanna with a tree cover of approximately 38 %, based on ground surveys at the site and satellite-based estimates in the 2006 National Land Cover Database (http://www.mrlc.gov). Measurements made using an optical Plant Canopy Analyzer (LAI-2000; Li-Cor, Lincoln, NE) indicated that the leaf area index (LAI) for pine crown cover is approximately three, which is typical for pine stands (Geron et al. 1994). A LAI of three and tree cover of 38 % leads to a stand averaged LAI of approximately 1.15. The open understory consists predominantly of bunchgrasses and forbs. Woody vegetation in the forest is almost exclusively ponderosa pine (*Pinus ponderosa* P. Lawson & C. Lawson subs. *scopulorum* Engelm.).

BVOC sample collection methods

During the summer of 2009, a total of 12 sets of needles were sampled at 30 °C and high irradiance (PPFD > 1,000 μmol m^{-2} s^{-1}). BVOC emissions from needles were characterized on approximately a weekly basis. In July and August, 2011, an additional six sets of needles were sampled under the same conditions. Needles begin to elongate in mid-June but reach a convenient length for sampling (>6 cm) only in late July. Thus, two thirds of the needles sampled were second-year needles and one third were newly emerged. Five or six fascicles of pine needles (generally three needles per fascicle; occasionally two) were enclosed in a custom built temperature-controlled, fan-stirred glass cuvette (Allen Scientific Glass, Boulder, CO) 12.5 cm in diameter (volume of 425 cm^3), which was tethered to a control console (MPH-1000, Campbell Scientific, Logan, UT). In all cases, the base of each fascicle and all woody tissue remained outside the enclosure and the enclosed tissue comprised only needles. Air entering the cuvette consisted of zero air mixed with pure CO_2 to a final CO_2 concentration of approximately 400 ppm and humidified to a dew point between 6 and 8 °C. All mixing flows were controlled using mass flow controllers (Model 825, Edwards High Vacuum International, Wilmington, MA) and the flow rate of air entering the cuvette, which varied between 0.0007 and 0.00075 mol s^{-1}, was measured with a mass flow meter (Model 831, Edwards High Vacuum International). Except where otherwise stated, leaf temperature was controlled to 30.0 ± 0.3 °C using thermoelectric coolers. In some experiments, the cuvette was illuminated using natural light; in others, light was provided by a 90-W LED (red/blue) growth lamp. Incident PPFD was measured with a photodiode (Hamamatsu), calibrated against a quantum sensor (Model SQ-110, Apogee Instruments, Logan, UT) and placed inside the cuvette adjacent to needles. A known volume of air exiting the cuvette, generally 4–6 liters, was collected at a rate of approximately 200 sccm onto stainless steel tubes packed with two adsorbents in series (Tenax GR or Tenax TA and Carbograph 5TD) using a small pump and a mass flow controller. The sorbent tube samples were then kept under refrigeration until analyzed in the laboratory.

In 2011, in an effort to better understand controls over terpenoid emissions and the possible importance of stomatal conductance, continuous measurements of net photosynthesis, stomatal conductance, and BVOC emission rates under fluctuating natural conditions were made on two sets of one-year old needles, each for approximately 24 h. Air exiting the leaf enclosure was directed to a Teflon© T-fitting, from which air was pulled by vacuum into the inlet of a proton transfer reaction mass spectrometer (PTR–MS) at a rate of approximately 20 sccm. In addition, a fraction of the air exiting the cuvette was diverted to a CO_2 and H_2O infrared gas analyzer (LI-6252, Li-Cor, Lincoln, NE), and rates of net photosynthesis, transpiration and stomatal conductance were calculated using the equations of von Caemmerer and Farquhar (1981). In addition to continuous PTR–MS measurements, approximately every 2 h, air exiting the leaf enclosure was collected onto sorbent tubes for subsequent analysis using GC–MS.

Additional measurements designed to investigate the importance of incident photosynthetic photon flux density (PPFD) and stomatal conductance in controlling BVOC emissions from ponderosa pine needles were made using a portable gas exchange system (LI-6400; LI-COR, Lincoln, NE). Needles were arranged in a tightly packed layer across the 6 cm^2 enclosure, and light was provided using the red-blue light emitting diode source. The default experimental conditions were 400 ppm CO_2 in air entering the cuvette, 1,000 μmol m^{-2} s^{-1} PPFD and needle temperature of 30 °C, but either the PPFD or the temperature could be varied to examine independently the light or temperature dependences of BVOC emissions. Air entering the enclosure was scrubbed of BVOCs using a platinum catalyst heated to 350 °C. Air exiting the enclosure was pulled from a T-fitting into the inlet of the PTR–MS for analysis of BVOCs.

All portions of needles within the enclosure were excised after measurement, oven-dried at 70 °C for 48 h or until no further weight loss was observed, and weighed. In 2011 only, total needle surface area was estimated as follows. All portions of needles within the enclosure were reassembled into individual fascicles of two or three needles. Fascicle length and diameter were measured using calipers and total needle surface area was then estimated assuming each needle formed either one half or one third of a cylinder, depending on the number of needles per fascicle. In addition, all fascicles were submerged in water in a small graduated cylinder and total water displacement, a

surrogate for total needle volume, was measured. Again, assuming cylindrical geometry, total needle surface area was estimated. In general, these two techniques agreed within 10 %.

In 2011, needle transpiration rates were calculated, and rates of BVOC emission on a leaf surface area basis (E_A, nmol m^{-2} s^{-1}) were calculated according to Eq. 1, incorporating the transpiration correction recommended by Niinemets et al. (2011).

$$E_A = (\sigma_{out} - \sigma_{in}) \times \frac{F_m}{A_L} + \lambda \times \sigma_{out}, \quad (1)$$

where σ_{in} and σ_{out} (nmol mol^{-1}) are mole fractions of the BVOC of interest in the air entering and exiting the enclosure, respectively, F_m is the molar flow rate (mol s^{-1}), A_L is total needle surface area (m^2), and λ is the transpiration rate (mol m^{-2} s^{-1}). In 2009, needle area was not determined and emission fluxes were expressed on a needle dry mass basis (E_M, μg g^{-1} h^{-1}) and without the transpiration correction.

Gas chromatography–Mass spectrometry analysis

Air samples collected onto sorbent cartridges were thermally desorbed at 275 °C using an Ultra autosampler (Series 2, model ULTRA TD, Markes International, Llantrisant, UK) and then cryofocused (0 °C) onto a Unity thermal desorber operated in splitless mode. The samples were desorbed from the cryotrap (300 °C) and injected into a gas chromatograph (GC; model 7890A, Agilent Technologies, Inc., Santa Clara, CA, USA) equipped with both a flame ionization detector (FID) and an electron impact mass-selective detector (MSD). An HP-5MS column (30 m × 0.25 mm, 0.25 μm, Agilent Technologies, Inc., Santa Clara, CA, USA) was used with nitrogen as the carrier gas. The GC oven program used was as follows: start temperature, −30 °C; 1 min hold; Ramp, 20 °C min^{-1} to 0 °C; Ramp 6 °C min^{-1} to 80 °C; Ramp 3 °C min^{-1} to 190 °C; Ramp 30 °C min^{-1} to 260 °C; and 6 min hold.

Low analyte masses in emission samples and the presence of coeluting peaks made peak quantitation using FID problematic. Thus, we developed a method to estimate analyte concentrations using the signal from the MSD in selected ion mode (SIM). In order to use the MSD signal for quantitation, one should have a response factor for each analyte of interest, which is based on a known concentration standard. Lacking a wide array of gas phase standards; however, we developed a protocol to estimate analyte concentrations.

Briefly, the peak area associated with the major ion fragment of each compound of interest (e.g., *m/z* 93 for all monoterpenes) was quantified in SIM mode. To account for changes in MSD sensitivity, a constant 2 ml volume of an internal standard, decahydronaphthalene (DHN), was included with all samples, and measured analyte signals were normalized using a similar mass fragment from DHN (e.g., MBO signals at *m/z* 71 were divided by the *m/z* 68 fragment of DHN and monoterpene signals at *m/z* 93 were divided by the *m/z* 95 fragment of DHN). For the purpose of calibration, several sorbent tubes loaded with a known mass of isoprene and camphene were included in each batch run, and the normalized signal (e.g., *m/z* 93 of camphene divided by *m/z* 95 of DHN) was related to the known mass of standard. This calibration factor could be used directly to quantify camphene peaks in the sample sorbent tubes, but the ratio of the *m/z* 93 fragment to the total ion count for other monoterpenes differs. Thus, the calibration factor for camphene was adjusted for use with other monoterpenes based on the reported (NIST) or empirically determined ratio of *m/z* 93 to total ion counts. This protocol is described in greater detail in the Electronic Supplementary Materials, together with some empirical tests of its validity.

The 2-methyl-3-buten-2-ol (MBO) dehydrates during thermal desorption, yielded variable amounts of isoprene (Harley et al. 1998). No emissions of isoprene from ponderosa pine have been reported, and we assume here that all isoprene measured in emission samples arose from the dehydration of MBO. However, a small contribution from directly emitted isoprene cannot be excluded. In addition to catalyzing the production of MBO, the enzyme MBO synthase is reported to catalyze small amounts of isoprene production, in a ratio of 90:1 (Gray et al. 2011) and small amounts of both isoprene and MBO can be produced non-enzymatically by acid-catalyzed solvolysis of dimethylallyl diphosphate that is the substrate from which both MBO and isoprene are derived (Sanadze 1991). Karl et al. (2012), using PTR–MS with NO^+ as the primary ion, were able to measure MBO and isoprene independently, and reported that isoprene was present in a small amount (90–250 pptv) in air above the forest, but we assume that this isoprene originated from sources other than ponderosa pine (e.g., willows, aspen or spruce upwind of the site). Assuming that direct emissions of isoprene from needles of ponderosa pine are negligible, our reported MBO emission rates were, therefore, obtained by summing the calculated masses of isoprene and MBO in each sample.

The relationship between myrcene and linalool is analogous to that of isoprene and MBO, i.e., the myrcene-linalool pair represents an exact C-10 structural analog of that C-5 pair, and myrcene is the dehydrated form of linalool. We have observed in laboratory tests with pure linalool samples a variable amount of conversion to myrcene during thermal desorption and analysis. Finally, the ^{13}C labeling patterns of the two compounds (described below) are almost identical. Thus, although we report myrcene and

linalool as separate emissions, we suspect that a significant fraction of reported myrcene arises from linalool dehydration during analysis.

$^{13}CO_2$ labeling experiments

$^{13}CO_2$ fumigation experiments were carried out to determine the extent of de novo production of terpenoids from recently fixed carbon. Needles were inserted into the chamber with a flow of air containing approximately 400 ppm CO_2 with a naturally occurring isotopic signature (1.109 % $^{13}CO_2$). Following the establishment of steady state emissions at 30 °C and high PPFD (1,000 μmol m^{-2} s^{-1}), a sorbent tube was collected for analysis using GC–MS. The CO_2 entering the chamber was then replaced with isotopically-labeled CO_2 (99 % ^{13}C, Sigma Aldrich, St. Louis, MO). Beginning 90 min after the introduction of $^{13}CO_2$, six additional sorbent tubes were collected at approximately 60 min intervals to characterize the incorporation of ^{13}C into the emitted terpenoid compounds.

Measurement of BVOCs using PTR–MS

The Proton Transfer Reaction Mass Spectrometer (Ionicon, Innsbruck, Austria) was operated as described previously (de Gouw and Warneke 2007). The 2-methyl-3-buten-2-ol (MBO, *m/z* 87) and total monoterpenes (*m/z* 137) were monitored continuously. The PTR–MS was calibrated using a gas standard that included known concentrations of MBO and α-pinene (used as the standard for monoterpenes).

Inducing stomatal closure using abscisic acid (ABA)

To elucidate the role of stomatal conductance in controlling BVOC emissions, experiments were carried out in which stomatal closure was induced by introducing abscisic acid (ABA) through the transpiration stream. A small branch was severed using a sharp blade and the cut end immediately placed in a beaker and recut under water in a 1 % methanol solution (required to dissolve ABA) to maintain a continuous transpiration flow. Needles were introduced into the LI-6400 enclosure and stomatal conductance and BVOC emissions monitored continuously. After approximately one hour, ABA was added to the beaker to make a 75 μM ABA solution, and changes in stomatal conductance and terpenoid emissions were then followed for 90 min.

Results

BVOC emissions from *P. ponderosa* were consistently dominated by MBO which comprised, on average, 87 % of total terpenoid emissions on a mass basis (mean emission rate at 30 °C and high irradiance was 18.0 ± 7.4 μg g^{-1} h^{-1}). Smaller, but significant, contributions came from monoterpenes (including alkyl benzenes such as p-cymene and p-cymenene) and oxygenated monoterpenes, primarily estragole (in Spring 2009 only) and linalool. Sesquiterpene emissions, primarily α- and β-farnesene and β-caryophyllene, were observed but comprised less than 1 % of the total terpenoid flux.

Emissions of unsubstituted monoterpenes were dominated by β-pinene, followed by α-pinene and the sum of limonene and β-phellandrene (which coeluted and could not be separated with confidence). Myrcene was frequently observed in relatively high concentrations but correlated strongly with emissions of linalool, and we suspect that a significant fraction of the myrcene results from dehydration of linalool during thermal desorption. Camphene and Δ-3-carene were always present in small amounts, and the alkyl benzenes, p-cymene and p-cymenene contributed significantly. Approximately 20 % of the total monoterpene emissions arose from generally small contributions of a large number of other compounds (α-thujene, sabinene, α-phellandrene, α-terpinene, γ-terpinene, terpinolene, 4-terpineol, and α-terpineol). *E*-β-ocimene was generally present in trace amounts, but on three sampling dates it comprised over 25 % of monoterpene emissions. Oxygenated monoterpenes made up a significant portion of the total flux throughout the measurement period (on average, they comprised approximately 75 % of the total C-10 terpenoid emission by mass), but the composition of the oxygenated fraction changed in mid-summer of 2009, with the development of new needles. Oxygenated BVOC in emission samples from needles produced in 2008 were dominated by estragole (methyl chavicol), whereas estragole was almost undetectable in elongating needles produced in 2009. Instead, the oxygenated fraction was dominated by linalool. Needles produced in 2010 and sampled in July–August 2011 emitted almost no estragole but they did emit substantial amounts of linalool.

Figure 1 depicts results from continuous measurements made on two sets of needles under naturally fluctuating light and temperature conditions (Fig. 1a, b) over the diurnal cycle. Continuous measurements of net photosynthesis and stomatal conductance (Fig. 1c, d) and BVOC emission rates, measured using PTR–MS, were made on two sets of needles and are also shown. MBO emissions (Fig. 1e, f) and total monoterpenoid emissions (Fig. 1g, h) are depicted separately. Approximately every 2 h, air exiting the leaf enclosure was collected onto sorbent tubes for subsequent analysis using GC–MS. MBO emission data from GC–MS analysis is included in Fig. 1e, f. Emissions of linalool are shown along with summed data from all other monoterpenoids as well as the total monoterpenoid flux for comparison with PTR–MS data (Fig. 1g, h).

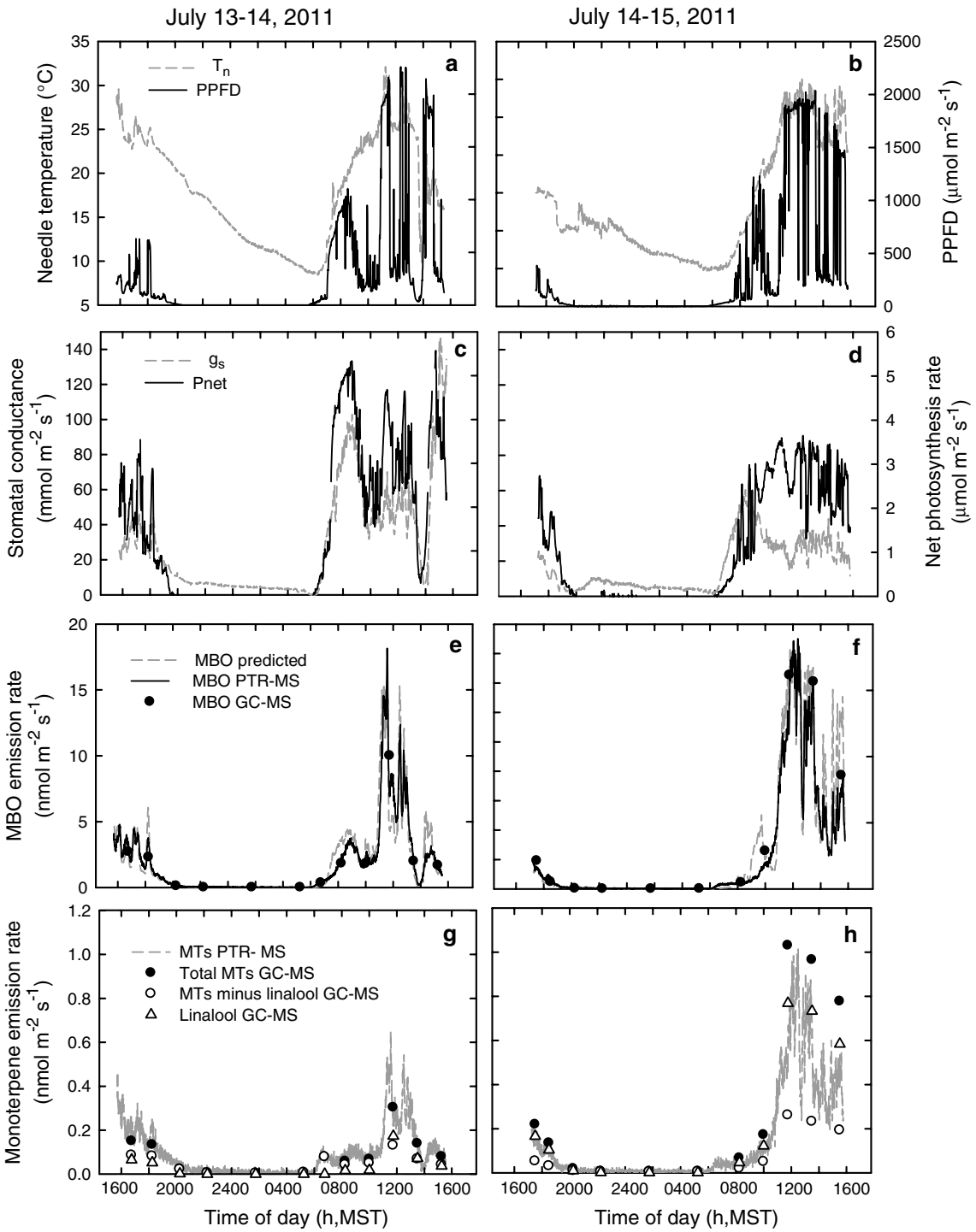

Fig. 1 Diurnal variation in environmental drivers, leaf gas exchange, and terpenoid emissions from two sets of ponderosa pine (*Pinus ponderosa* subs. *scopulorum*) needles. **a**, **b** Depict needle temperature (*dashed grey line*) and incident PPFD (*solid line*), **c**, **d** illustrate net photosynthesis (*solid line*) and stomatal conductance (g_s, *dashed grey line*). **e, f** Show continuous MBO emission data collected using PTR–MS (*solid line*) as well as discrete samples collected onto sorbent tubes and analyzed by GC–MS (*filled symbols*). Also shown are emissions predicted by the model of Niinemets and Reichstein (2003a) (*dashed grey line*). **g**, **h** Show continuous total monoterpenoid data collected using PTR–MS (dashed grey line) and GC–MS (*filled circles*); the GC–MS data is further divided into linalool emissions (*open triangles*) and all other monoterpenoid emissions (open circles)

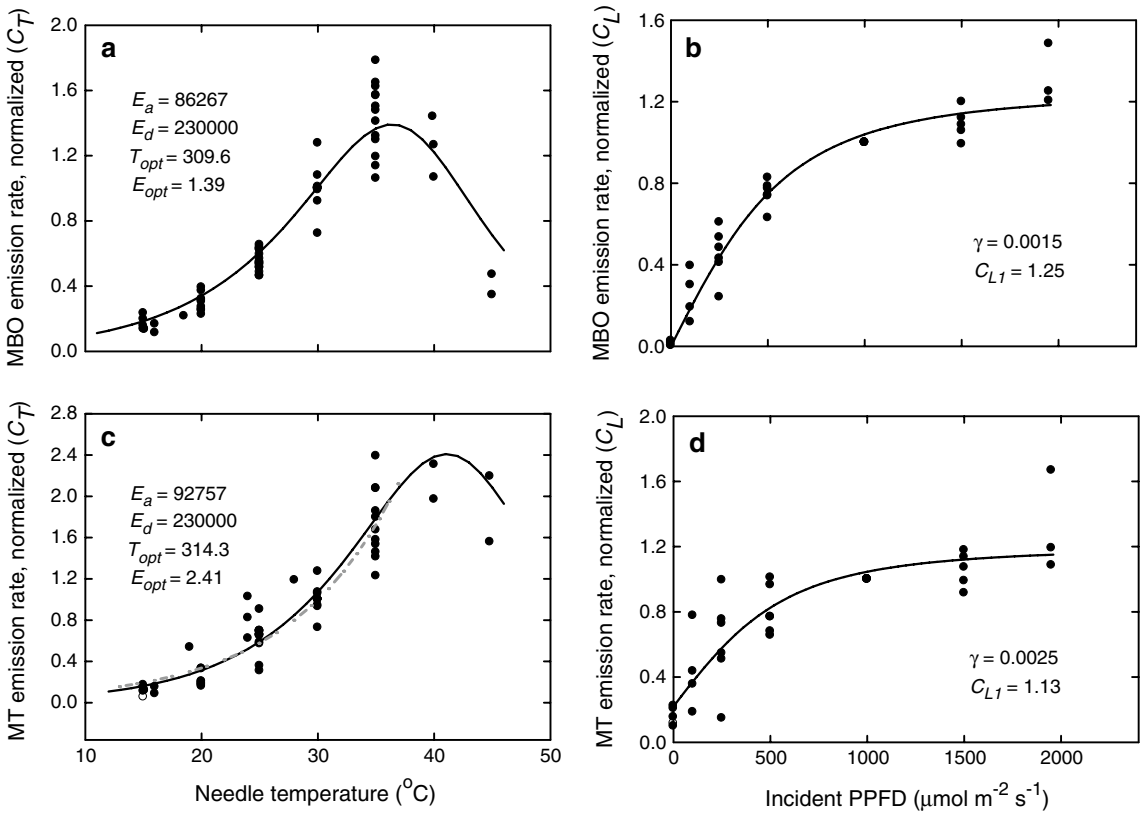

Fig. 2 Data depicting the temperature and light dependences of MBO and total monoterpenoid emissions, incorporated into Eq. 2 as C_T and C_L, respectively. **a, c** Illustrate, respectively, the temperature dependence of C_T for MBO and total monoterpenoid emissions ($n = 10$), with data normalized to the value measured at 30 °C. **b, d** Illustrate the light dependence of C_L for MBO and total monoterpenoid emissions ($n = 6$), with data normalized to the value measured at PPFD = 1,000 μmol m^{-2} s^{-1}. The *solid line* in **a** and **c** represents the best least-squares fit to Eq. 3, using the parameters shown. Data in **c** between 15 °C and 35 °C were also fit to Eq. 5 (*dashed line*) using a value of β = 0.109. The *solid line* in **b** and **d** represents the best least-squares fit to Eq. 4, using parameter values shown

Modeling these diurnal emissions requires information about the physical controls over the production and emission of individual BVOC. The rate of BVOC production, E, is modeled as follows:

$$E = E_{30,1000} \times C_T \times C_L, \quad (2)$$

where $E_{30,1000}$ is the steady state emission rate under standard conditions of 30 °C and PPFD = 1,000 μmol m^{-2} s^{-1}. C_T and C_L are scalars, which account for the effects of needle temperature and incident PPFD, respectively, and which take on values of 1.0 at standard conditions. In the absence of any light dependence on BVOC production, or when emissions result solely from diffusion out of storage structures such as resin canals, C_L takes on a constant value of 1.0.

In order to characterize C_T and C_L, dependence of BVOC emissions on needle temperature and incident PPFD was measured. Five experiments relating MBO emission to needle temperature (incident PPFD > 1,000 μmol m^{-2} s^{-1}) were carried out using sorbent tubes and GC–MS. An additional five experiments, in which temperature was varied over a more limited range (25–35 °C), were analyzed using PTR–MS. All data were normalized by assigning a value of 1.0 to the measured emission rate at 30 °C and scaling other rates proportionally (Fig. 2a). Emissions of MBO increase exponentially with temperature before leveling off, and then decline as temperature continues to increase. The temperature scalar, C_T, is described using Eq. 3, a temperature function developed to model emissions of isoprene (Guenther et al. 1993) that has been successfully used to model MBO emissions (Harley et al. 1998):

$$C_T = \frac{E_{\text{opt}} E_d \exp^{E_a x}}{E_d - E_a(1 - \exp^{E_d x})}, \quad (3)$$

where $x = [(1/T_{\text{opt}}) - (1/T)]/R$, T is needle temperature (K), R is the gas constant (=8.314 J mol^{-1}), T_{opt} is the temperature optimum (K), E_{opt} is the normalized emission rate at T_{opt} (unitless), and E_a and E_d are the energies of activation and deactivation (J mol^{-1}), respectively. The least-squares fit to the normalized temperature data is shown in Fig. 2a, along with best-fit values of E_a, T_{opt} and E_{opt} (E_d was fixed at 230,000 J mol^{-1}, since a paucity of data above the temperature optimum precludes accurate estimation).

Curves relating MBO emissions to incident PPFD were obtained from six sets of needles using the LI-6400 and PTR–MS. Leaf temperature was held constant at 30 °C and PPFD was varied between 0 and 2000 μmol m^{-2} s^{-1}. Data were normalized by assigning the measured emission rate obtained at PPFD = 1,000 μmol m^{-2} s^{-1} a value of 1.0 and scaling other data accordingly (Fig. 2b). The scalar describing the effects of incident PPFD, C_L, is described by Eq. 4, developed by Guenther et al. (1993) to model emissions of isoprene, but also used previously to model MBO emissions (Harley et al. 1998):

$$C_L = \frac{\gamma C_{L1} L}{\sqrt{1 + \gamma^2 L^2}}, \quad (4)$$

where L is incident PPFD, and γ (m^2 s μmol photons^{-1}) and C_{L1} (unitless) are empirical coefficients. The equation was fit to the data in Fig. 2b and best-fit values of γ and C_{L1} are shown.

Data relating total monoterpene emissions to needle temperature were obtained on six sets of needles using the LI-6400 and PTR–MS (*m/z* 137) and on five sets of needles collecting samples on sorbent tube for GC–MS analysis. All identified monoterpenes and oxygenated monoterpenes with emission rates greater than 0.01 μg g^{-1} h^{-1} were summed to estimate "total monoterpenoid" emissions. As with MBO, monoterpene data were normalized to a temperature of 30 °C (Fig. 2c). It has long been recognized that monoterpene fluxes increase exponentially with temperature, a relationship formalized by Guenther et al. (1993):

$$C_T = \exp^{\beta \times (T-303)}, \quad (5)$$

where T is needle temperature (°K) and β is an empirical coefficient (°K^{-1}). When these fluxes represent diffusion out of specialized storage structures such as resin canals in ponderosa pine, this temperature dependence reflects the increase in terpene vapor pressure with temperature. Because this is a purely physical process, emissions from pools are expected to increase indefinitely until high temperatures cause damage to the storage structures. However, our data indicate that the relationship between total monoterpene emissions and temperature exhibits a temperature optimum, above which emissions decline. This behavior suggests that monoterpenoid emissions in ponderosa pine do not result entirely from diffusion out of resin canals, but that some fraction of emissions arises from de novo production, in which case a temperature optimum would be observed, analogous to the situation for MBO (Fig. 2a). This interpretation is supported by ^{13}C labeling results reported below. We therefore chose to fit the normalized data of total monoterpene emissions to Eq. 3, with E_d again set to 230,000 J mol^{-1}. The results are shown by the solid black line in Fig. 2c, using best-fit parameter values shown, and this description of the temperature response is used in the modeling exercises to follow. For comparison with other published data on the temperature dependence of monoterpenoid emissions, the fit to the data between 15 and 35 °C using Eq. 5 is also shown ($\beta = 0.109$).

Because the observed response of total monoterpene emissions to temperature was consistent with a significant amount of de novo production, we screened for a light dependence on monoterpene emissions by measuring emissions at 30 °C in the light (PPFD = 1,000 μmol m^{-2} s^{-1}) followed by emissions after a period in darkness, and then followed by a return to high light (examples are given in Supplemental Materials). Each time the light was changed, a 30 min period was allowed for equilibration prior to beginning sample collection, which occurred over the following hour. We calculated for each compound the percentage of total emissions that appeared to be dependent on light [i.e., 100 × (emissions in light minus emissions in darkness) divided by emissions in light] as an indicator of the responsiveness of each emitted compound to light. These values ranged from 0 % (no light dependence) to 91 % for light-dependent MBO (Table 1, column [b]). The response of individual monoterpenes to darkening varied widely. Emissions of α-pinene and β-pinene, camphene, limonene, and Δ-3-carene exhibited only slight, if any light dependency (0–17 %). Values for all other terpenoid species exceeded 35 %, suggesting some degree of light dependence, with the value exceeding 60 % for the oxygenated monoterpene linalool and several other monoterpenes including sabinene, myrcene (at least some of which likely arises from dehydration of linalool during thermal desorption), α-terpinene and γ-terpinene, *E*-β-ocimene, terpinolene, and the sesquiterpene β-farnesene.

Based on these observations, total monoterpenoid emissions measured using PTR–MS would be expected to evince a light dependency, the magnitude of which would depend on the mix of terpenoids comprising the total. This light dependence of total monoterpenoid emissions was confirmed, based on measurements of total monoterpenes using the LI-6400 and PTR–MS while varying incident PPFD at a constant enclosure temperature of 30 °C (Fig. 2d). Given the presence in the monoterpene mixture of a significant amount of α-pinene and β-pinene, emissions of which were largely independent of light, emissions did not fall to zero in the dark, although the fact that dark emissions were only 25 % of high light emissions suggests the presence of a large fraction of light-dependent monoterpenes in the mixture, especially the oxygenated monoterpene, linalool. The light response data of monoterpene emissions was, therefore, modeled assuming that 25 % of the total was independent of light, while Eq. 4 was used to simulate the remaining 75 % with the best-fit parameters indicated in Fig. 2d.

Complicating the interpretation of the light dependency of both MBO and total monoterpenoid emissions is the fact that

Table 1 Light dependence and ^{13}C labeling of terpenoid emissions from needles of ponderosa pine and Austrian pine

Terpenoid	*Pinus ponderosa*				*Pinus nigra*			
	% Light-dependent emissions	% ^{13}C label	Emission rate (nmol m^{-2} s^{-1})	De novo emission (nmol m^{-2} s^{-1})	% Light-dependent emissions	% ^{13}C label	Emission rate (nmol m^{-2} s^{-1})	De novo emission (nmol m^{-2} s^{-1})
[a]	[b]	[c]	[d]	[e]	[f]	[g]	[h]	[i]
MBO	91	100	6.933	6.933	96	90.6	0.58	0.522
α-Thujene	62	29.4	0.0014	0.0004	99	90.4	0.019	0.017
α-Pinene	17	2.3	0.163	0.0037	81	47.7	0.20	0.095
Camphene	0	1.9	0.05	0.0009	77	32.0	0.016	0.005
Sabinene	74	52.5	0.002	0.0010	98	95.7	0.051	0.048
β-Pinene	9	0.3	0.471	0.0014	88	34.0	0.041	0.014
Myrcene[a]	90	78.5	0.098	0.0769	98	96.3	0.287	0.276
α-Phellandrene	50	35.3	0.0003	0.0001	97	77.3	0.0025	0.002
Δ-3-carene	9	0.2	0.154	0.0003	–	–	–	–
α-Terpinene	69	53.7	0.0006	0.0003	96	87.2	0.001	0.001
p-Cymene	–	36.9	0.0031	0.0012	–	–	–	–
Limonene	17	26.9	0.084	0.0226	93	77.4	0.039	0.030
β-Phellandrene	38	17.4	0.056	0.0097	–	–	–	–
1,8-Cineole	–	–	–	–	94	100	0.863	0.863
Z-β-Ocimene	52	27.5	0.019	0.0052	–	–	–	–
E-β-Ocimene	76	69.4	0.002	0.0014	93	–	–	–
γ-Terpinene	62	62.3	0.001	0.0006	95	94.8	0.006	0.006
Terpinolene	68	35.7	0.0043	0.0015	–	–	–	–
p-Cymenene	17	27.5	0.0018	0.0005	93	–	–	–
Linalool	71	70.3	0.412	0.2896	93	65.7	0.054	0.036
4-Terpineol	–	–	–	–	88	42.7	0.007	0.003
α-Terpineol	57	–	–	–	82	21.3	0.230	0.048
β-Caryophyllene	–	–	–	–	47	4.0	0.002	0
β-Farnesene	76	87.3	0.0005	0.0004	83	56.0	0.0013	0.001

Columns [b] and [f] indicate for each terpenoid the percentage of emissions which are dependent on light, calculated as 100 x (light emissions – dark emissions) divided by light emissions, where all measurements were conducted at 30 °C and PPFD for light emissions was 1,000 μmol m^{-2} s^{-1}. Columns [c] and [g] present the percentage of ^{13}C-labeled following a six-hour exposure to $^{13}CO_2$ under conditions of 30 °C and PPFD = 1,000 μmol m^{-2} s^{-1}, following the protocol of Ghirardo et al. (2010) and assuming MBO was fully labeled in ponderosa pine and 1,8-cineole was fully labeled in Austrian pine. Assigning them a value of 100 %, all other compounds were scaled accordingly. Column [d] and [h] present the measured emission rate of each compound prior to labeling (nmol m^{-2} s^{-1}) and columns [e] and [i] provide rough estimates of the labeled emission rate (nmol m^{-2} s^{-1}) presumed to derive from de novo synthesis and obtained by multiplying columns [c] and [d] for *P. ponderosa* and [g] and [h] for *P. nigra*

[a] Assumed in *P. ponderosa* to result in large part from the dehydration of linalool

stomatal conductance generally declines rapidly with decreasing PPFD. This raises the possibility that at least some of the observed reductions in emission as PPFD is lowered may be the indirect result of decreasing stomatal conductance.

In order to determine whether there was a direct effect of light on de novo terpenoid production, we conducted ^{13}C-labeling studies using the same needles used in the light versus dark study described above. If emissions of a given terpenoid result exclusively from diffusion out of preexisting pools sequestered in specialized storage structures, replacing $^{12}CO_2$ in the air entering the needle enclosure with $^{13}CO_2$ should not result in short-term changes in the isotopic signature of the emitted compound. In contrast, those terpenoids not found in storage pools, such as isoprene or MBO, should rapidly acquire ^{13}C label, the final ratio of unlabeled to labeled emissions reflecting the percentage of product arising from old rather than newly fixed carbon, which is typically about 20 % for isoprene (Karl et al. 2002).

During GC–MS analysis, very little of the protonated parent mass of MBO (*m/z* 87) is observed because most

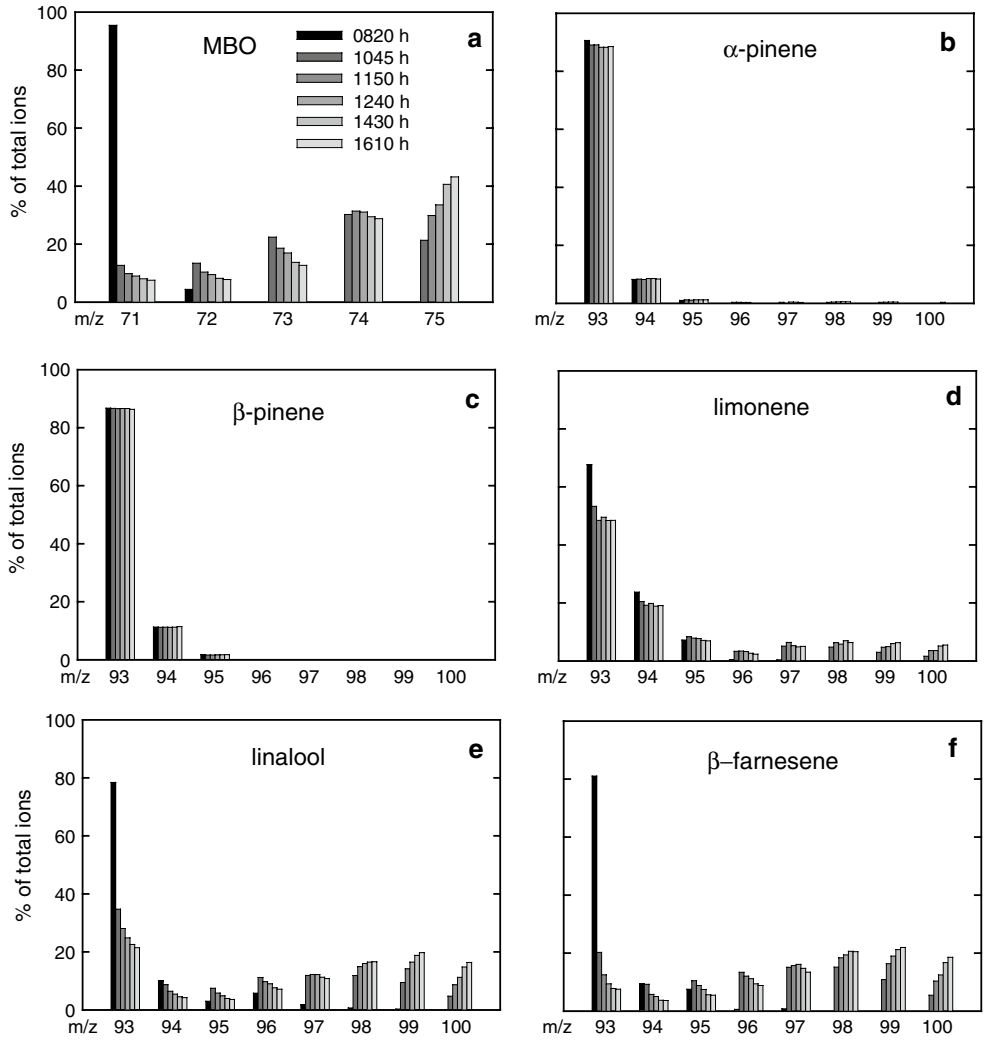

Fig. 3 Results of an experiment to characterize the uptake of ^{13}C by various terpenoids emitted by needles of ponderosa pine during continuous exposure to $^{13}CO_2$. The *y*-axis depicts the percentage of the total ion spectrum arising from each of the possible *m/z* signals associated with the dominant fragment for a particular terpenoid, which are indicated on the *x*-axis. Thus, the fully unlabeled 4-C fragment of MBO will have *m/z* 71; if one C atom is ^{13}C, it will appear as *m/z* 72, etc., up to a fully-labeled *m/z* 75. The change in the percentage of a given *m/z* over time is illustrated by the series of bars, with the left bar associated with each *m/z* representing the percentage prior to the introduction of $^{13}CO_2$. The additional bars, moving from left to right, represent a time series of sample collections following the beginning of labeling with the mid-point of the sample collection time shown in the legend. Note that all monoterpenoids were characterized by the major 7-C fragment at *m/z* 93

of the MBO fragments. The dominant observed mass (*m/z* 71) arises from a four carbon fragment. Labeling of one to four of the carbon atoms with ^{13}C gives rise to heavier fragments at *m/z* 72, 73, 74 and 75. Prior to exposure to $^{13}CO_2$, approximately 95.4 % of the MBO signal derived from *m/z* 71, and approximately 4.4 % from *m/z* 72, which is consistent with the 1.1 % $^{13}CO_2$ in ambient air and the four carbon atoms in the fragment (Fig. 3a, 8:20 am). As expected for light-dependent MBO, following the switch to air containing $^{13}CO_2$, the signal at *m/z* 71 decreased rapidly, leveling off at approximately 8 % of the total mass spectrum, and each of the four carbon atoms rapidly became labeled with the heavier isotope, which demonstraties de novo production (Fig. 3a). Six hours after introduction of $^{13}CO_2$, the percent of ^{13}C in the final emission sample was 74 %, implying that 26 % of the carbon originates from sources other than recently fixed carbon. Since MBO is not stored within the leaf, and following Ghirardo et al. (2010), we consider MBO fully labeled, and assign it a value of 100 %, and scale all other compounds accordingly (Table 1, column [c]). Thus, a compound with 37 % of its carbon atoms labeled at the conclusion of the experiment would be considered 50 % labeled (i.e., 37 % divided by 74 %).

The labeling of individual monoterpenes is more complex, reflecting emissions from both storage pools and de novo production. If compounds are produced de novo from recently fixed carbon, their emissions should acquire some ^{13}C label; however, the degree to which emissions of a given compound become labeled will depend both on the rate of de novo production and the magnitude of the flux of unlabeled compound from storage pools in the resin canals (Ghirardo et al. 2010). For α-pinene or β-pinene, for example, which comprise a large fraction of the monoterpene storage pool (Greenberg et al. 2012), the extent of labeling may remain low even if there is de novo production because any ^{13}C-labeled de novo emissions will be diluted by the large amount of unlabeled emissions from storage.

Fluxes of α-pinene and β-pinene from the needles used in this experiment, measured prior to labeling, were relatively high (0.163 and 0.471 nmol m^{-2} s^{-1}, respectively; Table 1, column [d]) and only slight changes in isotopic composition of emissions of either α-pinene (Fig. 3b) or β-pinene (Fig. 3c) were observed over the six hours of labeling. Only 2.3 % of α-pinene emissions were ^{13}C enriched and only 0.3 % of β-pinene emissions (Table 1, column [c]), which provides evidence that almost all emissions represented diffusion of unlabeled compounds from resin canals. Nevertheless, if 2.3 % of α-pinene emissions became labeled, this represents a de novo flux of 0.0037 nmol m^{-2} s^{-1} (2.3 % of 0.163 nmol m^{-2} s^{-1}) (Table 1, column [e]). Similarly, 0.3 % of 0.471 nmol m^{-2} s^{-1} represents a de novo flux of 0.0014 nmol m^{-2} s^{-1} of β-pinene. Similar labeling patterns were observed for camphene and Δ-3-carene. Both of them are significant components of the monoterpene storage pool, and both of them showed only slight ^{13}C enrichment of emissions from de novo production (Table 1).

Estimates of de novo flux of all emitted monoterpenes are given in Table 1, column [e], but it should be emphasized that these are highly uncertain, especially for those compounds with very low emission rates.

The labeling situation for the remaining monoterpene emissions differed, as other terpenes with much lower emission rates became labeled to a far greater extent with ^{13}C, although the degree of labeling varied. Sabinene, for example, became rapidly labeled, and the final samples were enriched by 52.5 % with measured emissions of only 0.002 nmol m^{-2} s^{-1}. The absolute amount of de novo sabinene emitted was 0.001 nmol m^{-2} s^{-1}, whiich is comparable to the absolute amounts of de novo α-pinene and β-pinene emissions. Similar patterns were observed for other monoterpenes (e.g., α-phellandrene, α-terpinene and γ-terpinene, *E*-β-ocimene, and terpinolene). All of them became over 35 % labeled; but all of them had emission rates less than 0.01 nmol m^{-2} $s^{-1,}$ and none of them was identified in needle pools (Greenberg et al. 2012) although several were very minor components of needle resin as reported by Smith (1977). The oxygenated monoterpene linalool (Fig. 3e) and myrcene, assumed to derive largely from dehydration of linalool, were unique in that they were emitted at high rates (0.412 and 0.098 nmol m^{-2} s^{-1}, respectively) and also became strongly labeled (70.3 and 78.5 %). Linalool was not a component of needle storage pools (Greenberg et al. 2012), evinced a strong light dependency, and it was assumed to derive solely from de novo production, as suggested previously (Niinemets et al. 2002).

An additional ^{13}C labeling experiment accompanied by a 'light on light off' comparison was carried out on needles of pine trees thought to be *P. ponderosa*, but subsequently identified as Austrian pine (*Pinus nigra*), which is a widely planted European species. Labeling of MBO (a significant emission in *P. nigra*, but much lower than *P. ponderosa*) was rapid and similar to that in ponderosa pine, but the labeling patterns of other BVOC from *P. nigra* differed in interesting ways (Table 1). The oxygenated monoterpene 1,8-cineole (eucalyptol), absent from needle resin (unpublished data), was the major emission from *P. nigra* needles and became over 76 % labeled (Supplementary Material, Fig. 2e), comparable to MBO and linalool and indicative of complete de novo production. The α-pinene and β-pinene, which acquired almost no label in *P. ponderosa*, became labeled in *P. nigra* up to 48 % and 34 % respectively, relative to 1,8-cineole (Supplementary Material, Fig. 2b, c) and also exhibited greater reductions in emissions in darkness. The percentage of total emissions, which appeared to be dependent on light in the light on:light off experiments, and the final % of ^{13}C labeling (relative to 1,8-cineole) are summarized in Table 1 (columns [f] and [g], respectively) for comparison with ponderosa pine data. These high percentages of labeling cannot be an artifact resulting from low emission rates from storage, since α-pinene and β-pinene comprised 62 % and 35 %, respectively, of the total terpene pool in needles, and the pools were in fact larger than those measured in *P. ponderosa*. In general, emissions from *P. nigra* showed a far greater degree of ^{13}C labeling and, thus, de novo production (Table 1, column [i]), as well as more pronounced reductions of emissions in darkness.

Evidence for stomatal control of emissions

Because BVOC emissions and stomatal conductance often covary in response to changes in PPFD, it can be difficult to determine unambiguously the controlling factor. The results above demonstrate that MBO and a significant fraction of the monoterpenoids observed in emissions of ponderosa pine are dependent on light, but this does not preclude the possibility that stomata may also limit diffusion of MBO and monoterpenes from either their sites of

production in the chloroplast or from specialized storage structures to the ambient air.

A straightforward method of determining whether emissions can be limited by stomata is to force stomatal closure by the introduction of abscisic acid (ABA) through the transpiration stream while maintaining incident PPFD and needle temperature constant. Results of such an experiment are illustrated in Fig. 4. When the needles were inserted into the LI-6400 chamber following the severing of the stem, stomatal conductance rapidly declined before recovering slightly after approximately 35 min. One hour after the stem was cut, ABA was added to the transpiration stream, stomata began to close, and within an hour, stomatal conductance had fallen to between 2 and 4 mmol m^{-2} s^{-1}. During the first 30 min following cutting, stomatal conductance dropped rapidly, and emissions of both MBO and total monoterpenes were little affected. Subsequently, during partial recovery from cutting the stem and then following the introduction of ABA, there was a close correspondence between stomatal conductance and both MBO and total monoterpenes (Fig. 4b, c).

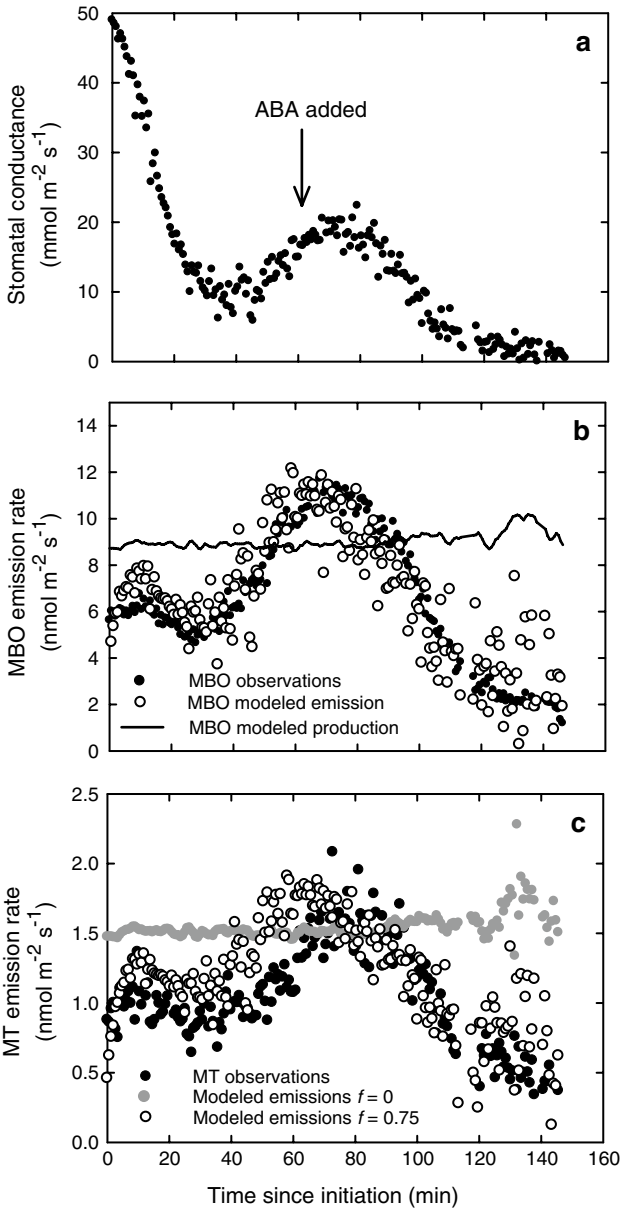

Fig. 4 Result of an experiment to establish whether stomatal conductance limits emissions of MBO and monoterpenoids from needles of ponderosa pine. A terminal branch was cut under water and measurements of stomatal conductance **a**, MBO **b** and total monoterpene emissions **c** commenced at time = 0. Abscisic acid (ABA) was added to the transpiration stream after approximately 65 min and emissions were followed as stomata closed. Also shown are the results of applying the dynamic model of Niinemets and Reichstein (2003a). Panel (**b**) shows rates of both modeled MBO production (*solid line*) and emission rate (*open circles*). Panel (**c**) depicts modeled emission rates with the parameter *f* (Eq. 6) assigned either a value of 0 (no de novo production; all monoterpenes assumed to have the physico-chemical characteristics of α-pinene; filled grey circles) or 0.75 (75 % of emissions arising from de novo production, assumed to have the physico-chemical characteristics of linalool; open circles)

Discussion

Ponderosa pine is a dominant tree species in many forested ecosystems of western North America. *Pinus ponderosa* var. *scopulorum* Engelm., the Interior or Rocky Mountain ponderosa pine, is a widespread variety (or subspecies) with a range extending from eastern Montana and the Dakotas through Wyoming and Nebraska into northern and central Colorado, Utah, and eastern Nevada. It forms extensive stands along the Colorado Front Range. The xylem resin composition of trees along the Front Range in Colorado is dominated by α-pinene and β-pinene, Δ-3-carene, limonene, and myrcene (Smith 1977), which is broadly consistent with our measurements of needle emissions. Minor xylem resin components included α-thujene, camphene, sabinene, β-phellandrene, γ-terpinene, and terpinolene. All of these were also observed in emissions from trees at the site. Observed as significant emissions, but absent from xylem resin, were the oxygenated monoterpenes estragole, terpineol, and linalool.

The primary aim of this study was to characterize terpenoid emissions at the needle scale and elucidate the environmental controls over those emissions. In particular, we sought to characterize the potential light dependency of the different monoterpene species emitted by ponderosa pine, and to determine the extent to which stomatal conductance might limit BVOC emissions. Ponderosa pine at

this site emit a variety of hemiterpenes, monoterpenes and sesquiterpenes with total emissions during daytime dominated by the hemiterpene, 2-methyl-3-buten-2-ol (MBO), comprising on average about 87 % of the terpenoid flux during periods of high irradiance. Emissions of unsubstituted monoterpenes contributed on average about 3 % of the daytime flux and are dominated by β-pinene, α-pinene, Δ-3-carene, and the sum of co-eluting limonene and β-phellandrene, although a large number of other monoterpenes made (usually) minor contributions. Small amounts of *E*-β-ocimene were generally observed, but on three sampling dates, *E*-β-ocimene emissions were quite large, comprising between 30 % and 40 % of the total monoterpene signal. *E*-β-ocimene is recognized as an important induced emission for plants undergoing herbivory (Arimura et al. 2009; Niinemets et al. 2013). Although we observed no significant herbivory during our study, we suspect these occasional enhanced emissions were in response to some type of biotic stress. Smith (1977) reported that myrcene was a minor component of xylem resin in ponderosa pine and significant quantities of myrcene were frequently observed in our emission samples. We report these emissions, but suspect that a significant fraction of reported myrcene arises from linalool dehydration during analysis, as discussed in Methods.

Emissions of oxygenated C_{10} species such as estragole (also known as methyl chavicol and not a terpenoid, being a product of the phenylpropanoid pathway) and linalool often comprised over 50 % of the daytime C_{10} BVOC flux, with additional contributions from several terpineol isomers.

Terpenoid flux measurements above Blodgett Forest, a ponderosa pine plantation in the foothills of the Sierra Nevada in California, were also dominated by MBO (Schade and Goldstein 2001). Bouvier-Brown et al. (2009a) measured emissions from branches in August 2005 and reported large branch emissions of estragole (8–54 % of the total monoterpenoids), but no linalool. In a subsequent paper (Bouvier-Brown et al. 2009b), they reported low mixing ratios of linalool (9.9 pptv in the air within the canopy and 0.74 pptv above the canopy) suggesting that ponderosa pine was a small source. The mix of emitted monoterpenes exhibited substantial tree to tree variability, but the dominant species in their study (α-pinene and β-pinene, Δ-3-carene, limonene + β-phellandrene, camphene, and myrcene) are consistent with data from our study. Minor constituents observed at our site (α-terpinene and γ-terpinene, terpinolene) were also observed in emissions at Blodgett Forest.

Our needle scale observations can be compared with results of above-canopy flux and atmospheric mixing ratio results from the BEACHON campaigns at the Manitou Experimental Forest Observatory site. Daytime terpenoid fluxes, measured using the eddy covariance technique and reported by Kaser et al. (2013a), were dominated by MBO with fluxes generally about five times those of monoterpenes. Following a damaging hail storm, emissions of monoterpenes increased markedly (4-fold to 23-fold). Above-canopy fluxes of sesquiterpenes were never observed, consistent with the low emission rates observed at the needle scale and the likelihood of scavenging within the canopy of these reactive species (Ciccioli et al. 1999).

Flux measurements using the relaxed eddy accumulation (REA) technique with sample analysis using GC–MS provide information on the speciation of emitted monoterpenoids. Although generally consistent with our needle observations, significant discrepancies were apparent, perhaps reflecting chemical transformations or removal or significant emissions from non-needle sources such as litter or woody tissues, or from exposed resin. The largest monoterpene fluxes above the canopy, of more or less equal magnitude, were α- and β-pinene and Δ-3-carene, with a significant contribution from limonene/β-phellandrene (Turnipseed et al., in prep.). Thus, Δ-3-carene, which comprised only a small fraction of needle monoterpene emissions, was a dominant component of the ecosystem flux. Strikingly absent from flux measurements above the canopy or air mixing ratio measurements above the canopy was linalool, even in late July–August when it comprised a large fraction of emissions from newly elongated needles. Thus, compared with our needle scale observations, air above the canopy was significantly enriched in Δ-3-carene and depleted in linalool.

Ciccioli et al. (1999) reported large losses of linalool (on the order of 70 %) when comparing enclosure measurements in a Valencia orange grove with fluxes above the canopy measured using the REA technique. The losses could not be explained based on known reaction rates of linalool with O_3 and other atmospheric oxidants, and they hypothesized that linalool may be lost by heterogeneous processes including partitioning into water droplets and adsorption on particles. Another possible reason for the inconsistency with respect to linalool in our data is the use of ozone filters, consisting of Pall® Acrodisc® glass fiber syringe filters (Sigma-Aldrich) impregnated with sodium thiosulfate on the air sampling inlet. Laboratory studies carried out at NCAR demonstrated that a large percentage of a linalool standard mixture was lost when passed through filter paper with a nominal pore size of 1 μm, whether or not it was impregnated with sodium thiosulfate or potassium iodide. In August 2013, we collected a series of ambient air samples from the flux tower. Some of them were pulled through an ozone trap and some of them used no trap. Ozone was removed from another set of samples using the technique pioneered by Arnts (2008) in which the incoming air sample is mixed with high

concentrations of *trans*-2-butene (~200 ppm) in order to titrate away any O_3. No linalool was observed in either the filtered or the unfiltered sample. Trace amounts of linalool were observed in the butene-titrated samples (<50 pptv) but far less than would be predicted on the basis of needle emissions. Roskamp (2013) collected ambient air samples in August 2011 and analyzed them using 2-D GC–MS and also reported small amounts of linalool, but again, considerably less than needle emissions would suggest. Neither reaction with O_3 nor reaction with the OH radical is sufficiently rapid to explain these observed losses. It is worth noting that both enclosure and ambient air measurements made at Blodgett Forest incorporated in line Pall A/E glass fiber filters (1 μm pore size) coated with sodium thiosulfate prior to analysis, and a copper mesh impregnated with MnO_2 was used to scrub O_3 in the REA measurements above the canopy made by Ciccioli et al. (1999), discussed above. However, the large inconsistency in our data between enclosure measurements and fluxes/concentrations above the canopy remains unexplained. Observations of unexpectedly high formaldehyde fluxes at the site (DiGangi et al. 2011) suggest that a significant amount of BVOC processing within the canopy was taking place, but its significance in the possible removal of linalool is unknown.

In addition to the absence of linalool, ambient air samples differed from needle emission samples in the relative proportion of monoterpene species. Not surprisingly, the minor constituents of the emission samples were not observed in the ambient air; however, the proportion of the dominant monoterpene species was markedly different from that observed in needle emissions. In particular, Δ-3-carene was frequently one of the dominant monoterpenes observed in ambient air samples or flux measurements above the canopy, whereas it typically comprised a relatively small fraction of the needle emission profile (on average, less than 5 %). This observation raises the possibility of a significant non-needle source of monoterpenes, enriched in Δ-3-carene relative to needles. Emissions from soils at the site comprised less than 1 % of the observed flux above the canopy (Greenberg et al. 2012) and could not explain this discrepancy. Eller et al. (2013) frequently observed small balls of resin at the site, forming at the base of fascicles (and not, therefore, enclosed in the leaf cuvettes), as well as large resin pools which form on woody tissues at wound sites. They found that monoterpene emissions from these resin balls, like those from needles, were comprised primarily of α-pinene and β-pinene, Δ-3-carene, and limonene + β-phellandrene, with Δ-3-carene comprising a much higher percentage of the total monoterpenes (over one third) than observed in needle emissions. BVOC emissions from woody tissues have not been measured at the site, but it is likely that any emissions arising from woody tissues will have a VOC composition similar to that of resin balls. Heijari et al. (2011) reported significant monoterpene emissions (also enriched in Δ-3-carene) from apparently undamaged stems of *Pinus sylvestris* (Scots pine) seedlings, and Amin et al. (2012) also found that undamaged stems of *Pinus contorta* var. *latifolia* (lodgepole pine) emitted monoterpenes. In each of these studies, stem emissions increased significantly when stems were damaged, by weevils in the case of *P. sylvestris* (approximately a three-fold increase) or bark beetles in lodgepole pine (five-fold to 20-fold increase). Although emissions from stems were not quantified in this study, six samples of air collected from Teflon bags placed around apparently undamaged trunks was analyzed by GC–MS and found to be significantly enriched in carene (39 ± 7 % of monoterpenes). Kim et al. (2010) measured branch level emissions at the Manitou site, which included emissions from entire fascicles and woody tissues, and reported that Δ-3-carene comprised about 17 % of the total monoterpene signal, which was significantly higher than from needles alone. They also found that Δ-3-carene contributed about 21 % of the total monoterpene fraction in ambient air. It appears likely that the high percentage of Δ-3-carene in ambient air is due in large measure to emissions from woody tissues or resin exudate, which apparently comprise a significant but unquantified percentage of the total BVOC flux from the forest. Since emissions from resin or woody tissue contain no linalool, this additional source would also result in lower percentages of linalool in ambient air than in needle emissions.

Elucidating environmental controls over MBO emissions

Figure 2 depicts two days (one day each on two sets of needles) of MBO emissions from ponderosa pine; measured with a combination of PTR–MS and GC–MS techniques, which were in good agreement, considering the temporal differences in sample collection (continuous for PTR–MS versus 20 min to half-hour averages for GC–MS). Modeling these diurnal emissions requires information about the physical controls over both production and emission. Previous studies have shown that emissions of MBO, like those of isoprene, are controlled largely by incident PPFD and temperature and can be successfully modeled by assuming that it is emitted immediately upon production. The rate of production has been successfully modeled based on measured emission responses to varying PPFD and temperature (Harley et al. 1998; Schade et al. 2000). In addition to establishing the effects of needle temperature and incident PPFD on MBO production, we sought to determine whether or not emission was simultaneous with production or whether changes in stomatal conductance also affected emissions.

Production of MBO is simulated using Eq. 2, with the scalars describing the response to needle temperature (Fig. 2a) and incident PPFD (Fig. 2b) modeled using Eqs. 3 and 4, respectively. Previous investigators have found that this simple model predicts emission behavior well (Harley et al. 1998). However, MBO is quite soluble in water ($H = 1.55$ Pa m^3 mol^{-1}) and is, therefore, susceptible to transient storage in the aqueous phase of the cell. As shown in Fig. 4a, forcing stomata to close using ABA can lead to reductions in MBO emissions even though production is assumed to remain constant given steady state conditions of PPFD and temperature.

It has been convincingly demonstrated that stomata cannot limit emissions of BVOC under steady state conditions (Monson and Fall 1989; Loreto et al. 1996). However, as first suggested by Niinemets and Reichstein (2002, 2003a, b) and corroborated since (see Harley 2013 for review), the aqueous and lipid phases within the cell constitute nonspecific storage pools, the size of which depends on leaf anatomy and, more importantly, the physico-chemical properties of each specific BVOC. Following a perturbation in production rate, the presence of temporary storage pools may delay the reestablishment of steady state conditions. Until steady state conditions are reestablished, stomatal conductance may limit the emission rate, regardless of whether a given BVOC is produced de novo and emitted immediately upon production or diffuses from specialized storage structures such as resin canals in ponderosa pine.

The Niinemets-Reichstein model assumes that the BVOC of interest is produced at some prescribed rate, controlled by temperature. For BVOCs whose production is known to be dependent on photon flux density, such as MBO, this dependence on production must also be included. The BVOC diffuses in the liquid phase along a series of diffusion pathways until it reaches the outer surface of the cell walls and the interface between aqueous and gas phases. At that point, liquid to gas phase partitioning is determined by H, the Henry's Law constant, and the BVOC in the gas phase diffuses into the substomatal cavity and then through the stomata and leaf boundary layer to the ambient air. Diffusion from the intercellular air space to the air outside the leaf boundary layer, i.e., the rate of emission, follows Fick's law, and is proportional to the partial pressure difference and the total gas phase conductance.

Assuming constant rates of BVOC production, i.e., no feedback inhibition on rates of production, any change in stomatal conductance is countered by a corresponding, but opposite, change in the gas phase pool, resulting in a change in the partial pressure gradient exactly proportional, but opposite in sign, to the change in conductance. Hence, there is no alteration in the flux. This is the case for the largely insoluble BVOCs, isoprene (Fall and Monson, 1992), and α-pinene (Loreto et al. 1996). However, highly soluble MBO partitions strongly into the liquid phase, and a large increase in liquid pool size following stomatal closure is required before gas partial pressure rises sufficiently to completely counteract the reduced conductance. Once a new equilibrium is reached, the original flux will be restored, but during this extended transition period to a new equilibrium state, stomata may have a significant impact on observed emissions.

All other things being equal, the extent to which stomata limit the flux of a given BVOC is determined largely by H. However, several other factors, including leaf anatomy, also influence the time needed for reequilbration of the leaf pools, helping to explain observed differences in stomatal sensitivity between species. Thus, in addition to H, the extent to which changes in stomatal conductance affect emissions is influenced by the magnitude of stomatal conductance, the rate at which stomata open or close, and by internal leaf anatomy, which determines resistances to intercellular diffusion in both gas and liquid phase and also establishes the potential liquid pool size. Full parameterization of the Niinemets-Reichstein model requires numerous anatomical assumptions, which affect internal diffusive resistances and the potential size of aqueous and lipid pools. For all our simulations, we have used the parameterization developed for *Pinus sylvestris* (Niinemets & Reichstein 2003b).

In Fig. 4b (open symbols), we apply the model to the data relating MBO emissions to ABA-induced changes in stomatal conductance. MBO production is assumed to depend on incident PPFD and temperature as described above, and remains essentially constant in the model at approximately 9.0 nmol m^{-2} s^{-1} except for a brief 1.5 °C temperature excursion at around 135 min. When the physico-chemical properties of MBO are included, however, modeled emissions closely track stomatal conductance, sometimes exceeding the rate of production as temporary storage pools empty and sometimes falling below production as pools fill. The correspondence between measurements and modeled results is quite good, demonstrating that the Niinemets-Reichstein model captures the importance of temporary storage pools in explaining short-term stomatal limitations.

Modeling diurnal emissions of MBO

Figure 5a, b reproduce the daytime MBO emissions depicted in Fig. 1e, f. In each panel, the solid line represents emission rates predicted by the model of Niinemets and Reichstein (2003a, b) described above. The value of $E_{30,1000}$ for each set of needles was obtained empirically by determining the value which provided the best overall fit to the data. In general, the MBO emissions predicted by the model were similar to the predicted rates of

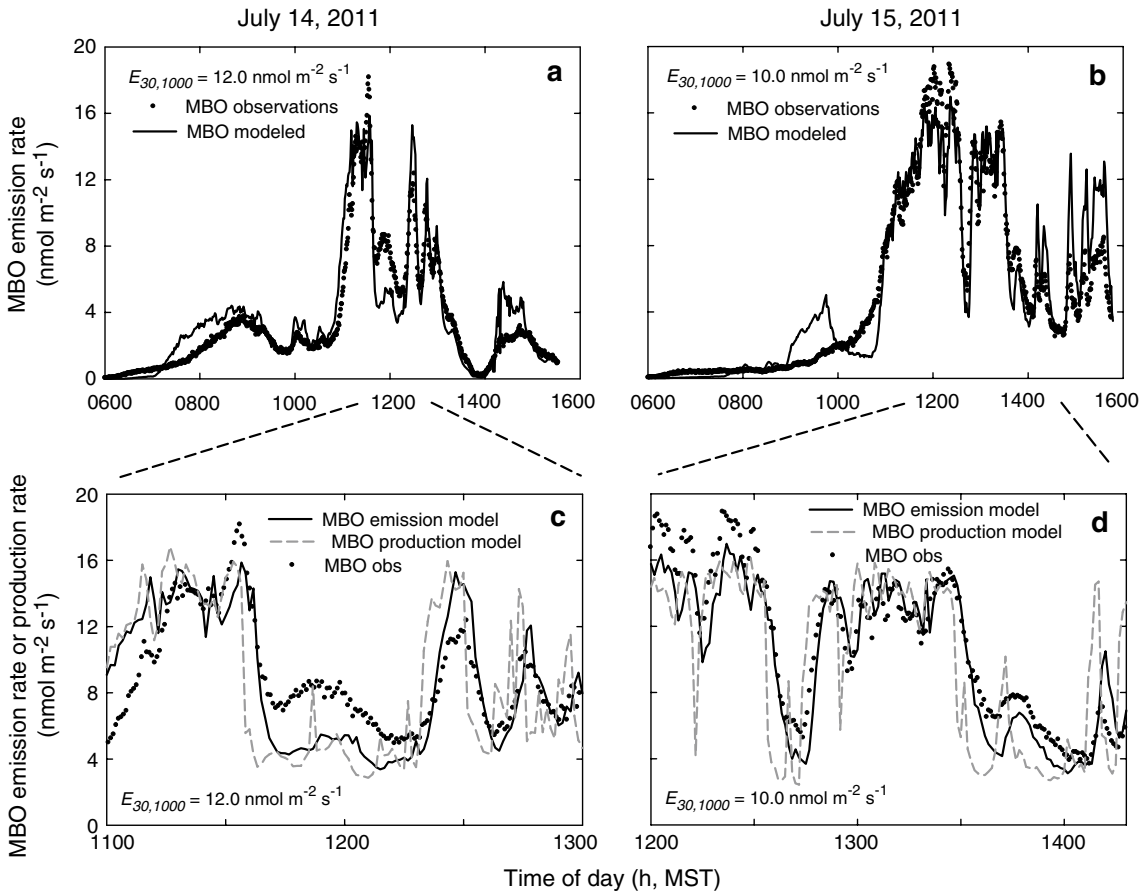

Fig. 5 Results of applying the dynamic model of Niinemets and Reichstein (2003a) to the MBO emission data shown in Fig. 1. **a** Model fit (*solid line*) to MBO emission data (*filled circles*) collected on 14 July, where production is modeled according to Eqs. 2, 3 and 4, using parameter values shown in Fig. 3a, b. The value of $E_{30,1000}$ was adjusted empirically to achieve the best overall fit to the observations. **b** Model fit to MBO emission data of 15 July. **c** Two-hour segment of data and model fit in (**a**), indicating the time lag between modeled rates of production (*grey dashed line*) and modeled emission rates (*solid line*). **d** Two-and-a-half hour segment of the data in (**b**)

production, implying only a minor role for transient storage. Only when the time resolution is increased by examining a two (Fig. 5c) or two-and-a-half hour (Fig. 5d) portion of the data when incident light was fluctuating, are the effects of storage and stomatal limitations apparent. As a result of its physico-chemical properties, MBO can temporarily reside in the aqueous phase of the leaf until a new gas–liquid phase equilibrium is reestablished. Thus, a slight delay is introduced between any change in the rate of MBO production (dashed grey line) and MBO emission. A similar lag is also apparent in response to changes in stomatal conductance. As a result, the simulated rates of emission lag slightly behind the predicted rate of production, providing a slightly improved fit to measured data compared with modeling emissions on the basis of production alone. Thus, although Figs. 4, 5c and d confirm that stomatal limitations can play a role in controlling the emissions of MBO, the effects under naturally fluctuating environmental conditions are subtle, affecting only the short-term (seconds-to-minutes) emission dynamics.

Elucidating environmental controls over monoterpenoid emissions

Until recently, monoterpene emissions from species with specialized storage structures, such as resin canals in pine needles were generally thought to be independent of light despite occasional reports that some monoterpenes are synthesized from recently assimilated carbon and subject to light dependence (e.g., Yokouchi and Ambe 1984; Schuh et al. 1997; Ortega et al. 2007). Schürmann et al. (1993) found that emission of both α-pinene and β-pinene from *Picea abies* was reduced by over 75 % in darkness and that both rapidly became labeled under $^{13}CO_2$ fumigation. Niinemets et al. (2002) reported that emissions of *E*-β-ocimene and linalool from needles of *Pinus pinea* were dependent on light, and, subsequently,

a variety of terpenoid emissions, including ocimene, linalool, and β-farnesene, have been shown to be induced by exposure to biotic or abiotic stress, and to be dependent on light. Recent evidence obtained using ^{13}C-labeling (Ghirardo et al. 2010) clearly indicate that a variable percentage of monoterpenes emitted from several different species of conifer, including Scots pine, was derived from recently fixed carbon, and that there was a direct effect of PPFD on emissions. Taipale et al. (2011) showed that canopy-scale monoterpene emissions from a Scots pine dominated forest evinced a light dependency. These data clearly indicate that monoterpene emissions from species with specialized storage structures can arise either from diffusion out of storage or from de novo production, but the relative importance of each pathway varies among taxa.

Ghirardo et al. (2010) proposed a hybrid emission model, as originally suggested by Schuh et al. (1997), in which those emissions arising from pools are controlled solely by temperature, while de novo emissions are jointly controlled by PPFD and temperature, i.e.,

$$E = E_{30,1000}[fC_T C_L + (1-f)C_T], \quad (6)$$

where f is the fraction of emissions arising from de novo synthesis. Ghirardo et al. (2010) assessed ^{13}C labeling using PTR–MS and did not examine the labeling pattern of individual monoterpenes species. Our results from *P. ponderosa* and *P. nigra* clearly show: (1) that the percentage of emissions arising from de novo production varies widely for individual monoterpene species, and (2) that the percentage of emission arising from de novo production for a given monoterpene (e.g., α-pinene or β-pinene) may be quite different for different species. For *P. ponderosa*, the large amount of variation in the proportion of de novo emissions of different monoterpenes is largely explained by variation in the magnitude of emissions from storage pools. Those monoterpenes found in highest concentrations in needle resin pools, α-pinene and β-pinene, camphene, and Δ-3-carene were labeled with ^{13}C to only a very minor extent. Any of the de novo production was diluted with emissions from storage. In contrast, those monoterpenes with very low emission fluxes tended to become labeled to a much greater degree, as very little dilution occurred, although absolute rates of de novo emissions are quite small (Table 1).

Our results are consistent with those of Ghirardo et al. (2010), indicating that monoterpene emissions derive from two sources, and that a hybrid emission model (Eq. 6) is appropriate. As shown below, such a hybrid model was necessary in order to successfully simulate the dynamics in emissions that we observed in this study. Such a hybrid model has been incorporated, for example, into the emission model MEGAN2.1 (Guenther et al. 2012).

The proportion of the total monoterpenoid emissions assumed to arise from de novo production was estimated by comparing the measured emissions of oxygenated monoterpenes, generally dominated by linalool, which demonstrates a strong light dependence (Figs. 4b, 5e) with the unsubstituted monoterpenes, dominated by α-pinene and β-pinene, camphene, and Δ-3-carene, none of which exhibited emissions that were strongly dependent on light. The GC–MS based emission data indicated that, averaged over the growing season, oxygenated monoterpenes comprised approximately 75 % of the total monoterpenoid emissions under high irradiance. The monoterpene light response data presented in Fig. 2d were, therefore, simulated assuming that 25 % of emissions were not dependent on light, and when conducting the modeling exercises below, we assigned a value of 0.75 to the parameter f in Eq. 6.

As was the case with MBO, the observed decline in monoterpenoid emissions as light decreases (Fig. 2d) was accompanied by similar reductions in stomatal conductance, obscuring the relative importance of the two factors. In the experiment in which stomata were forced to close by the introduction of ABA, changes in monoterpenoid emission closely paralleled those of MBO, and clearly indicated that, under these conditions, stomata could limit total monoterpenoid emissions while production presumably remained constant (Fig. 4c). We modeled these results using the dynamic model of Niinemets and Reichstein (2003a, b). Attempts to model these data, assuming that all emitted monoterpenoids were unsubstituted monoterpenes with physico-chemical properties of α-pinene (i.e., f in Eq. 6 equals zero), failed to mimic observations (Fig. 4c). Because α-pinene is practically insoluble in water (H = 10,840 Pa m^3 mol^{-1}), there is no temporary storage within the aqueous phase of the needles and emissions closely track the rate of production. Based on GC–MS data, we assumed that 75 % of the observed emissions arise from de novo production of monoterpenoids having the physico-chemical properties of linalool. With a Henry's constant of 2.08 Pa m^3 mol^{-1}, linalool is almost as water soluble as MBO, and like MBO, can reside temporarily in aqueous phase storage pools, as shown previously by Noe et al. (2006). Under these assumptions, the model simulation conforms much more closely to the measured data (Fig. 4c) and emissions are clearly limited by stomatal conductance under these experimental conditions.

Modeling monoterpenoid diurnal emissions

Figure 6a, b reproduces the total monoterpene emission data from Fig. 1g, h. When attempting to model these diurnal patterns of monoterpenoid emissions, one also has to apply the hybrid model (Eq. 6) in which a large fraction of the emissions (f) is assumed to be produced

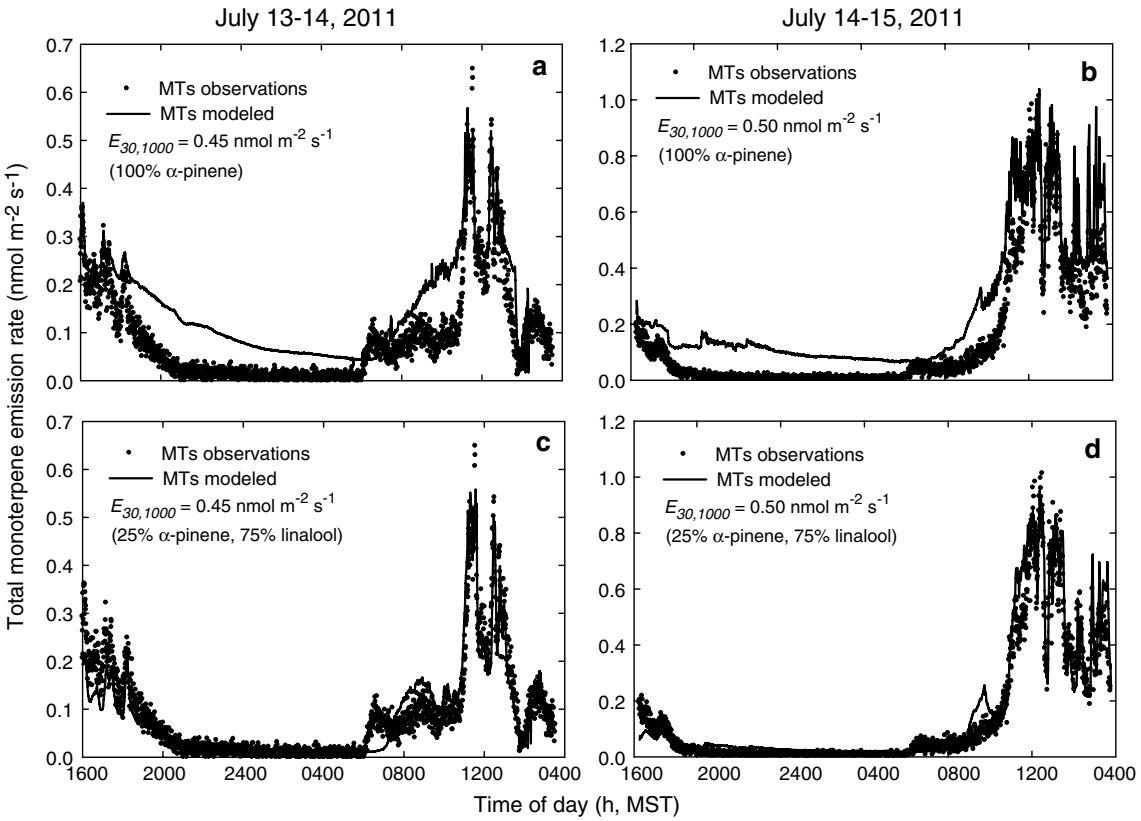

Fig. 6 Results of applying the dynamic model of Niinemets and Reichstein (2003a, b) to the monoterpenoid emission data shown in Fig. 1. **a** Model fit (*solid line*) to monoterpenoid emission data (*closed circles*) of July 13–14, where production is modeled according to Eqs. 2, 3, and 4, using parameter values shown in Fig. 2c, d. It is assumed that *f* (Eq. 6) is 0 and all monoterpenoid emissions arise from storage pools with no de novo production. The value of $E_{30,1000}$ was adjusted empirically to achieve the best overall fit to the observations. **b** Model fit to monoterpenoid emission data of July 14–15, as in (**a**). **c** As in (**a**) but *f* (Eq. 6) set to 0.75. (**d**) As in (**b**) but *f* set to 0.75

and emitted de novo and is both light and temperature dependent while the remainder (1−*f*) is dependent only on temperature. The temperature dependency of the de novo fraction is modeled using Eq. 3, parameterized as shown in Fig. 2c, while the emissions from storage pools in resin canals are modeled using the exponential function shown in Eq. 5 and a β value of 0.109 (Fig. 2c). Guenther et al. (1993) reported a range of empirical estimates of the parameter β (Eq. 5), which ranged from 0.062 to 0.144 (K^{-1}) with a mean of 0.09, a value which has been widely used since, although MEGAN2.1 (Guenther et al. 2012) uses a value for β of 0.1. The light dependency of the de novo fraction is modeled using Eq. 4, parameterized as shown in Fig. 2d.

Figure 6 depicts results obtained using the Niinemets and Reichstein (2003a, b) model, assuming two different values of *f*. The result assuming that all the monoterpenoid emissions behave like α-pinene and result from diffusion out of resin canals and are independent of light (i.e., $f = 0$ and C_L in Eq. 4 is set equal to 1) is shown for both sets of needles in Fig. 6a and b. As above with MBO, the best-fit value of $E_{30,1000}$ was determined empirically for each day and is shown on the figures. Clearly, the model overestimates emissions during periods of low light (late afternoon and early morning) as well as during the entire nighttime period. Three emission samples obtained on the afternoon of July 15 using GC–MS were analyzed and linalool comprised an average of approximately 72 % of the entire monoterpenoid fraction, consistent with our earlier decision to assign a value of 0.75 to the parameter *f*. Based on this assumption, the modeled rate of total monoterpenoid production provides a much improved fit to the measured data (Fig. 6c, d).

To address the question of whether stomata can limit monoterpenoid emissions under natural conditions of varying temperature and fluctuating light, we examined in greater detail a two hour or two-and-a-half hour segment of the data (Fig. 7). A comparison of modeled rates of production in the Niinemets and Reichstein model (dashed grey line) with measured emissions indicates that emissions frequently lag behind production by five to ten min, suggesting the presence of temporary storage pools within the leaf,

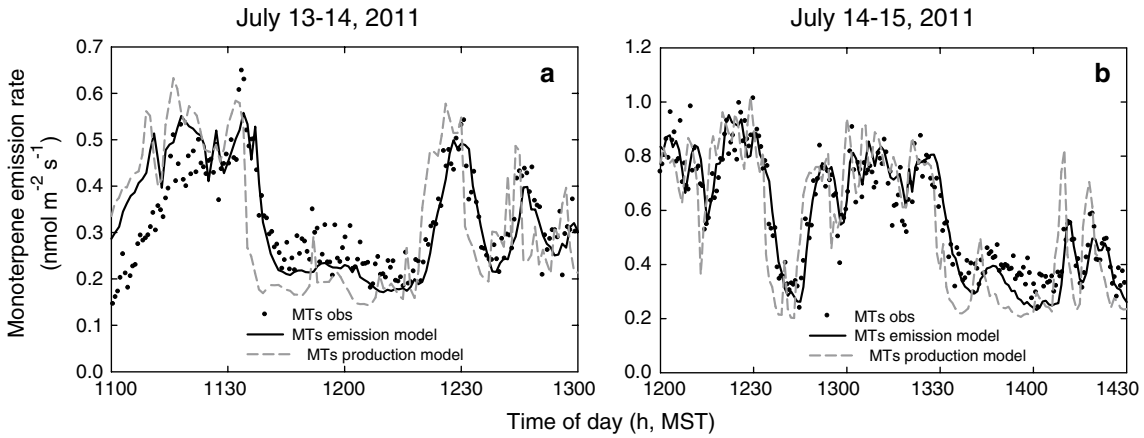

Fig. 7 Short segments of the data presented in Fig. 6 to illustrate finer details of the modeling exercise. **a** A 2-h segment of the data and model fits depicted in Fig. 6c illustrating the time lag between modeled rates of production (*dashed grey line*), modeled emission rates (*solid line*) and measured data (*closed circles*). **b** A two and one-half hour segment of the data and model fits depicted in Fig. 6d illustrating the time lag between modeled rates of production (*dashed grey line*), modeled emission rates (*solid line*) and measured data

analogous to the situation for MBO. Linalool, comprising 75 % of the $E_{30,1000}$ in these examples, with a Henry's constant of 2.08 Pa m^3 mol^{-1}, is only slightly less water soluble than MBO. Using the model of Niinemets and Reichstein (solid lines), which incorporates the physico-chemical properties of the produced terpenoids, significantly reduces the time lag between measured and modeled emissions and improves the overall fit. As was the case with MBO, the effect of introducing physico-chemical BVOC properties is to improve the temporal match between model and measured data over relatively short time periods of a few minutes, but the modeled emissions, integrated over tens of minutes, will be unaffected by stomatal changes.

Conclusions

Emissions of terpenoids from ponderosa pine are dominated by 2-methyl-3-buten-2-ol (MBO), and the diurnal emission variations are well described by existing algorithms describing the response of emissions to photon flux density and temperature. Experiments in which stomata were forced to close, however, indicate that under certain conditions, MBO emissions can be under stomatal control, consistent with the past studies of Niinemets and Reichstein (2003a, b). MBO, which is highly water soluble, partitions into the aqueous phase of the leaf; following a change in the rate of production or in stomatal conductance, there will be a period of non-steady-state emissions that will persist until the gas and liquid pools reach a new equilibrium. During this period, stomata can limit emissions. This behavior is well captured by the Niinemets-Reichstein model. While this phenomenon affects the short-term (seconds-to-minutes) dynamics of emissions, it does not affect the total MBO emissions integrated over longer time periods (hours-to-days).

Monoterpenoid emissions from needles of ponderosa pine exhibit a dependency on incident photon flux density, suggesting that a significant fraction of emissions arises from de novo production rather than from diffusion out of storage pools. Labeling experiments using $^{13}CO_2$ clearly demonstrate that the percentage of de novo emissions varies widely for different terpenoids. However, those monoterpenes which became only slightly labeled were those comprising the largest fraction of the needle storage pools and those with the highest absolute emission rates, suggesting that the low percentage of labeled emissions arises as a result of dilution by high emissions of nonlabeled compound from resin canals. In *P. ponderosa*, the only compound absent from needle pools but with high emission rates (only in the light) and a high degree of ^{13}C labeling is linalool, which, therefore, appears to be entirely dependent on light. Since linalool contributes up to 75 % of the monoterpenoid flux in high light, the total monoterpenoid flux is dependent on light, confirmed by simple light on:light off experiments. When attempting to model the diurnal pattern of monoterpenoid emissions from ponderosa pine, it is therefore necessary to use a hybrid monoterpenoid production model, in which a fraction of terpenoids is produced as a function of temperature alone, and the remainder depends on both light and temperature. Since linalool is water soluble and comprises a major fraction of the monoterpenoid flux, total monoterpenoid emissions can also be under stomatal control, as described for MBO.

Above-canopy flux or concentration measurements at the research site failed to detect significant amounts of linalool, suggesting losses within the canopy, sampling

difficulties or both. On the other hand, air above the canopy was enriched in Δ-3-carene relative to needle emission samples, suggesting the existence of a large non-needle source enriched in carene. Emissions from woody tissues and resin were both significantly enriched in Δ-3-carene, and may represent such a source. Additional studies examining the importance of these emissions are clearly called for.

Acknowledgments The National Center for Atmospheric Research is sponsored by the US National Science Foundation. RKM acknowledges support from NSF Grant 0919189.

References

Amin H, Atkins PT, Russo RS, Brown AW, Sive B, Hallar AG, Huff Hartz KE (2012) Effect of bark beetle infestation on secondary organic aerosol precursor emissions. Environ Sci Technol 46:5696–5703

Arimura G, Matsui K, Takabayashi J (2009) Chemical and molecular ecology of herbivore-induced plant volatiles: Proximate factors and their ultimate functions. Plant Cell Physiol 50:911–923

Arnts RR (2008) Reduction of biogenic BVOC sampling losses from ozone via trans-2-butene addition. Environ Sci Technol 42:7663–7669

Bouvier-Brown NC, Holzinger R, Palitzsch K, Goldstein AH (2009a) Large emissions of sesquiterpenes and methyl chavicol quantified from branch enclosure measurements. Atmos Environ 43:389–401

Bouvier-Brown NC, Goldstein AH, Gilman JB, Custer WC, de Gouw JA (2009b) *In-situ* ambient quantification of monoterpenes, sesquiterpenes, and related oxygenated compounds during BEARPEX 2007: implications for gas- and particle-phase chemistry. Atmos Chem Phys 9:5505–5518

Ciccioli P, Brancaleoni E, Frattoni M, Di Palo V, Valentini R, Giampero T, Seufert G, Bertin N, Hansen U, Csiky O, Lenz R, Sharma M (1999) Emission of reactive terpene compounds from orange orchards and their removal by within-canopy processes. J Geophys Res 104:8077–8094

de Gouw J, Warneke C (2007) Measurements of volatile organic compounds in the earth's atmosphere using proton-transfer-reaction mass spectrometry. Mass Spectrom Rev 26:223–257

DiGangi JP, Boyle ES, Karl T, Harley P, Turnipseed A, Kim S, Cantrell C, Maudlin RL III, Zheng W, Flocke F, Hall SR, Ullmann K, Nakashima Y, Paul JB, Wolfe GM, Desai AR, Kajii Y, Guenther A, Keutsch FN (2011) First direct measurements of formaldehyde flux via eddy covariance: implications for missing in-canopy formaldehyde sources. Atmos Chem Phys 11:10565–10578

Eller ASD, Harley P, Monson RK (2013) Potential contribution of exposed resin to ecosystem emissions of monoterpenes. Atmos Environ 77:440–444

Fall R, Monson RK (1992) Isoprene emission rate and intercellular isoprene concentration as influenced by stomatal distribution and conductance. Plant Physiol 100:987–992

Geron CD, Guenther AB, Pierce TE (1994) An improved model for estimating volatile organic compound emissions from forests in the eastern United States. J Geophys Res 99:12773–12791

Ghirardo A, Koch L, Taipale R, Zimmer I, Schnitzler J-P, Rinne J (2010) Determination of de novo and pool emissions of terpenes from four common boreal/alpine trees by $^{13}CO_2$ labelling and PTR–MS analysis. Plant, Cell Environ 33:781–792

Gray DW, Breneman SR, Topper LA, Sharkey TD (2011) Biochemical characterization and homology modeling of methylbutenol synthase and implications for understanding hemiterpene synthase evolution in plants. J Biol Chem 286:20582–20590

Greenberg JP, Asensio D, Turnipseed A, Guenther AB, Karl T, Gochis D (2012) Contribution of leaf and needle litter to whole ecosystem BVOC fluxes. Atmos Environ 59:302–311

Guenther AB, Zimmerman PR, Harley PC, Monson RK, Fall R (1993) Isoprene and monoterpene emission rate variability: Model evaluations and sensitivity analyses. J Geophys Res 98:12609–12617

Guenther AB, Jiang X, Heald CL, Sakulyanontvittaya T, Duhl T, Emmons LK, Wang X (2012) The Model of Emissions of Gases and Aerosols from Nature version 2.1 (MEGAN2.1): an extended and updated framework for modeling biogenic emissions. Geosci. Model Dev. 5:1471–1492

Harley PC (2013) The roles of stomatal conductance and compound volatility in controlling the emission of volatile organic compounds from leaves. In: Niinemets Ü, Monson RK (eds) Biology, controls and models of tree volatile organic compound emissions. Springer, Berlin, pp 181–208

Harley P, Fridd-Stroud V, Greenberg J, Guenther A, Vasconcellos P (1998) Emission of 2-methyl-3-buten-2-ol by pines: A potentially large natural source of reactive carbon to the atmosphere. J Geophys Res 103:25479–25486

Heijari J, Blande JD, Holopainen JK (2011) Feeding of large pine weevil on Scots pine stem triggers localised bark and systemic shoot emission of volatile organic compounds. Environ Exp Bot 71:390–398

Karl T, Fall R, Rosenstiel TN, Prazeller P, Larsen B, Seufert G, Lindinger W (2002) On-line analysis of the $^{13}CO_2$ labeling of leaf isoprene suggests multiple subcellular origins of isoprene precursors. Plant 215:894–905

Karl T, Hansel A, Cappellin L, Kaser L, Herdlinger-Blatt I, Jud W (2012) Selective measurements of isoprene and 2-methyl-3-buten-2-ol based on NO^+ ionization mass spectrometry. Atmos Chem Phys 12:11877–11884

Kaser L, Karl T, Guenther A, Graus M, Schnitzhofer R, Turnipseed A, Fischer L, Harley P, Madronich M, Gochis D, Keutsch FN, Hansel A (2013a) Undisturbed and disturbed above-canopy ponderosa pine emissions: PTR–TOF–MS measurements and MEGAN 2.1 model results. Atmos Chem Phys 13:11935–11947

Kaser L, Karl T, Schnitzhofer R, Graus M, Herdlinger-Blatt IS, DiGangi JP, Sive B, Turnipseed A, Hornbrook RS, Zheng W, Flocke FM, Guenther A, Keutsch FN, Apel E, Hansel A (2013b) Comparison of different real time BVOC measurement techniques in a ponderosa pine forest. Atmos Chem Phys 13:2893–2906

Kim S, Karl T, Guenther A, Tyndall G, Orlando J, Harley P, Rasmussen R, Apel E (2010) Emissions and ambient distributions of Biogenic Volatile Organic Compounds (BVOC) in a ponderosa pine ecosystem: interpretation of PTR–MS mass spectra. Atmos Chem Phys 10:1759–1771

Loreto F, Ciccioli P, Cecinato A, Brancaleoni E, Frattoni M, Tricoli D (1996) Influence of environmental factors and air composition on the emission of α-pinene from *Quercus ilex* leaves. Plant Physiol 110:267–275

Martin MJ, Stirling CM, Humphries SW, Long SP (2000) A process-based model to predict the effects of climatic change on leaf isoprene emission rates. Ecol. Modell. 131:161–174

Monson RK, Fall R (1989) Isoprene emission from aspen leaves: Influence of environment and relation to photosynthesis and respiration. Plant Physiol 90:267–274

Niinemets Ü, Reichstein M (2003a) Controls on the emission of plant volatiles through stomata: Differential sensitivity of the emission rates to stomatal closure explained. J Geophys Res 108:4208. doi :10.1029/2002JD002620

Niinemets Ü, Reichstein M (2003b) Controls on the emission of plant volatiles through stomata: a sensitivity analysis. J Geophys Res 108:4211. doi:10.1029/2002JD002626

Niinemets Ü, Reichstein M, Staudt M, Seufert G, Tenhunen JD (2002) Stomatal constraints may affect emission of oxygenated monoterpenoids from the foliage of *Pinus pinea*. Plant Physiol 130:1371–1385

Niinemets Ü, Kuhn U, Harley PC, Staudt M, Arneth A, Cescatti A, Ciccioli P, Copolovici L, Geron C, Guenther A, Kesselmeier J, Lerdau MT, Monson RK, Peñuelas J (2011) Estimations of isoprenoid emission capacity from enclosure studies: measurements, data processing, quality and standardized measurement protocols. Biogeosciences 8:2209–2246

Niinemets Ü, Kännaste A, Copolovici L (2013) Quantitative patterns between plant volatile emissions induced by biotic stresses and the degree of damage. Frontiers Plant Sci. doi:10.3389/fpls.2013.00262

Noe SM, Ciccioli P, Brancaleoni E, Loreto F, Niinemets Ü (2006) Emissions of monoterpenes linalool and ocimene respond differently to environmental changes due to differences in physicochemical characteristics. Atmos Environ 40:4649–4662

Ortega J, Helmig D, Guenther A, Harley P, Pressley S, Vogel C (2007) Flux estimates and OH reaction potential of reactive biogenic volatile organic compounds (BVOC) from a mixed northern hardwood forest. Atmos Environ 41:5479–5495

Ortega J, Turnipseed A, Guenther AB, Karl TG, Day DA, Gochis D, Huffman JA, Prenni AJ, Levin EJT, Kreidensweis SM, DeMott PJ, Tobo Y, Patton EG, Hodzic A, Cui YY, Harley PC, Hornbrook RS, Apel EC, Monson RK, Eller ASD, Greenberg JP, Barth MC, Campuzano-Jost P, Palm BB, Jiminez JL, Aiken AC, Dubey MK, Geron C, Offenberg J, Ryan MG, Fornwalt PJ, Pryor SC, Keutsch FN, DiGangi JP, Chan AWH, Goldstein AH, Wolfe GM, Kim S, Kaser L, Schnitzhofer R, Hansel A, Cantrell CA, Mauldin RL, Smith JN (2014) Overview of the Manitou Experimental Forest Observatory: site description and selected science results for 2008 to 2013. Atmos Chem Phys 14:6345–6367

Roskamp M (2013) Characterization of secondary organic aerosol precursors using two-dimensional gas chromatography-time of flight mass spectrometry (GCA x GC-TOFMS). Masters Thesis. Department of Civil and Environmental Engineering. Portland State Univ. http://pdxscholar.library.pdx.edu/cgi/viewcontent.cgi?article=2410&context=open_access_etd

Sanadze GA (1991) Isoprene effect—Light-dependent emissions of isoprene by green parts of plants. In: Sharkey TD, Holland EA, Mooney HA (eds) Trace gas emissions by plants. Academic Press, San Diego, pp 135–152

Schade GW, Goldstein AH (2001) Fluxes of oxygenated volatile organic compounds from a ponderosa pine plantation. J Geophys Res 106:3111–3123

Schade GW, Goldstein AH, Gray DW, Lerdau MT (2000) Canopy and leaf level emissions of 2-methyl-3-buten-2-ol from a ponderosa pine plantation. Atmos Environ 34:3535–3544

Schuh G, Heiden AC, Hoffmann T, Kahl J, Rockel P, Rudolph J, Wildt J (1997) Emissions of volatile organic compounds from sunflower and beech: Dependence on temperature and light intensity. J Atmos Chem 27:291–318

Schürmann W, Ziegler H, Kotzias D, Schönwitz R, Steinbrecher R (1993) Emission of biosynthesized monoterpenes from needles of Norway spruce. Naturwissenschaften 80:276–278

Smith RH (1977) Monoterpenes of ponderosa pine xylem resin in western United States. USDA Forest Service Tech. Bull. No. 1532, 48 pp

Staudt M, Seufert G (1995) Light-dependent emissions of monoterpenes by Holm oak (Quercus ilex, L.). Naturwissenschaften 82:89–92

Taipale R, Kajos MK, Patokoski J, Rantala P, Ruuskanen TM, Rinne J (2011) Role of de novo biosynthesis in ecosystem scale monoterpene emissions from a boreal Scots pine forest. Biogeosciences 8:2247–2255

von Caemmerer S, Farquhar GD (1981) Some relationships between the biochemistry of photosynthesis and the gas exchange of leaves. Planta 153:376–387

Yokouchi Y, Ambe Y (1984) Factors affecting the emission of monoterpenes from red pine (*Pinus densiflora*) – Long-term effects of light, temperature and humidity. Plant Physiol 75:1009–1012

Zimmer W, Bruggemann N, Emeis S, Giersch C, Lehning A, Steinbrecher R, Schnitzler J-P (2000) Process-based modelling of isoprene emission by oak leaves. Plant, Cell Environ 23:585–595